IEEE Access
Multidisciplinary : Rapid Review : Open Access Journal

Received August 19, 2020, accepted September 8, 2020, date of publication September 10, 2020, date of current version September 23, 2020.

Digital Object Identifier 10.1109/ACCESS.2020.3023342

Licensed Countrywide Full-Spectrum Allocation: A New Paradigm for Millimeter-Wave Mobile Systems in 5G/6G Era

RONY KUMER SAHA
Radio and Spectrum Laboratory, KDDI Research, Inc., Saitama 356-8502, Japan
e-mail: ro-saha@kddi-research.jp

ABSTRACT The traditional static allocation of a portion of the licensed spectrum specified for a country to a mobile network operator (MNO) is no longer sufficient to address the required spectrum demand, as well as efficient to utilize the allocated spectrum. To overcome these constraints, i.e. to increase the spectrum availability and utilization, in this paper, we present a new paradigm for the spectrum allocation called licensed countrywide full-spectrum allocation (LCFSA) to allocate the licensed countrywide full 28 GHz millimeter-wave (mmWave) spectrum to each MNO of a country to operate its small cells per building subject to avoiding co-channel interference (CCI). Since most data is generated indoors, the countrywide full mmWave spectrum allocated to an MNO is considered reusing further to its in-building small cells. CCI avoidance in both the time-domain and frequency-domain is presented along with deducing the conditions for optimality. We derive average capacity, spectral efficiency (SE), energy efficiency (EE), and cost efficiency (CE) for LCFSA, and perform extensive numerical and simulation results and analyses for a country consisting of four MNOs. It is shown that LCFSA with both the time-domain and frequency-domain CCI avoidance schemes provide similar performance improvement in average capacity, SE, EE, and CE by about 296%, 164%, 75%, and 60% respectively for no interfering user equipments (UEs), whereas by about 59.2%, 6.1%, 37.2%, and 0.45% respectively for all interfering UEs with the frequency-domain CCI scheme. Moreover, it is found that the improvement in the above metrics does not change with the spectrum reuse factor (RF) and the number of buildings of small cells per macrocell L, and the impact of interfering UEs can be compensated by adjusting RF. Finally, we show that LCFSA can satisfy the SE and EE requirements for sixth-generation (6G) systems by adjusting either RF or L, or both.

INDEX TERMS 28 GHz, 5G, 6G, millimeter-wave, mobile network operator, small cells, spectrum allocation, spectrum utilization, co-channel interference, countrywide, licensed.

I. INTRODUCTION

A. BACKGROUND

The ever-increasing user demand for the rich multimedia services, consuming a large data volume, and requiring a high data rate, causes existing mobile network operators (MNOs) to face challenges from the available radio spectrum allocated to them. Over time, even though the number of mobile subscribers and the introduction of new types of applications and services have been increased, the licensed spectrum allocated to an MNO in a country has not been increased in accordance. Such trends continue to grow, which in turn causes to grow the scarcity of a sufficient amount of available licensed spectrum for an MNO to address its user demand.

Another major challenge for an MNO in a country is to enable efficient utilization of its available licensed spectrum. This is because the user traffic demand of different MNOs in a country varies abruptly over time and space such that the demand for the required amount of spectra for different MNOs varies accordingly. This causes a great portion of the available spectrum allocated to each MNO in a country to be left unused or underutilized either in time or space. In this regard, since most data is generated indoors, particularly in dense urban multistory buildings, serving a large volume of data at high rates indoors causes these above challenges even more critical. Hence, increasing the available spectrum of

The associate editor coordinating the review of this manuscript and approving it for publication was Xingwang Li.

an MNO in one hand and improving the utilization of its spectrum on the other hand is crucial to maximizing serving its increased user demand at high data rates, particularly in dense urban multistory buildings.

In this regard, millimeter-wave (mmWave) bands are considered as promising candidates to address both the spectrum availability and utilization. MmWave bands offer a large amount of bandwidth [1] that can address the scarcity of radio spectrum. A major feature of mmWave systems is the dominance of the line-of-sight (LOS) components in the propagating signals because of the quasi-optical propagation characteristics [2]. In a pure LOS mmWave channel, a high data rate of 1-100 Gbps can be achieved [3]. Moreover, the mmWave spectrum can allow service providers to expand the channel bandwidth beyond 20 MHz used in the fourth generation (4G) systems, which results in supporting the increased data rates [4]. Furthermore, because of the very small wavelengths and advances in low-power complementary metal-oxide-semiconductor (CMOS) radio-frequency circuits, a large number of miniaturized antennas can be placed in small areas of less than 1 or 2 cm^2 to achieve very high gain, which can be either fabricated at the base station (BS) or in the skin of a mobile device to provide path diversity from the blockage by human obstructions [1].

Besides, MNOs continue to reduce cell coverage to exploit spatial reuse [4]. In this regard, to address the massive deployments of small cells to provide high data rates at a short distance, the short-range (typically, 100-200 m in radius) mmWave technologies are considered promising [5], particularly in urban indoor environments. Moreover, due to the high external wall penetration loss of a building, mmWave signals cannot penetrate easily, resulting in isolating indoor networks from that in outdoors [4]. Such isolations allow reusing the same outdoor mmWave spectrum indoors with an insignificant co-channel interference effect, resulting in an improved mmWave spectrum utilization. Furthermore, because of the availability of a large amount of the mmWave spectrum, a single MNO may not be able to utilize the mmWave spectrum fully. In such cases, sharing the mmWave spectrum dynamically among multiple operators in a country can contribute to improving further the utilization of the mmWave spectrum [1].

Note that though the mmWave spectrum is defined as the spectrum ranging from 30 GHz to 300 GHz that is mostly underutilized [5], any frequency above 10 GHz can be loosely considered as mmWave [1]. Moreover, the spectral allocations in the mmWave are relatively much closer than that below 3 GHz. This results in similar propagation characteristics of different mmWave bands unlike those below 3 GHz where the spectral allocations are sparse enough such that the cell coverage varies considerably at different bands [4].

B. RELATED WORK AND PROBLEM STATEMENT

Traditionally, a portion of the licensed spectrum specified for a country is allocated exclusively in a static manner to each MNO for a long term, which, however, is no longer considered sufficient to address the required spectrum demand, as well as efficient enough to utilize the allocated licensed spectrum for the MNO. To overcome these constraints associated with the static licensed spectrum allocation to an MNO, numerous approaches have already been proposed to address both the spectrum enhancement and spectrum utilization issues. In this regard, direct approaches such as the primary-level spectrum aggregation and the secondary-level spectrum trading, whereas indirect approaches such as spectrum sharing and spectrum reusing, have been considered effective and recommended in the existing literature to increase the amount, as well as the utilization, of the available spectrum of an MNO.

In spectrum aggregation such as carrier aggregation, the available spectrum of an MNO is increased by combining multiple component carriers in the same or different frequency bands to expand the available bandwidth to increase the peak data rate, as well as overall network capacity [6]–[8]. Carrier aggregation provides efficient spectrum utilization by combining multiple carrier signals [8]. In line with so, the authors in [9] have reviewed and analyzed the key challenges of realizing carrier aggregation techniques. Likewise, in [10], the authors have evaluated the performances of carrier aggregation schemes in Long-term Evolution-Advanced (LTE-Advanced) mobile systems. Moreover, in [11], the authors have investigated carrier aggregation and scheduler structures and proposed an idea of an improved scheduler structure for carrier aggregation.

Besides, the authors in [12] have addressed the multi-user multiple-input multiple-output (MIMO) resource scheduling of the LTE-Advanced system with carrier aggregation. It is to be noted that in massive MIMO systems, a BS is equipped with a large number of antennas (e.g., a few hundred or thousands antennas [13]) to serve tens of users sharing the same time-frequency resources [14]. Multiple data streams, which are precoded before transmitting based on the channel responses, are sent from the BS to user equipments (UEs) using the spatial-division multiplexing (SDM) technique [15]. By achieving considerable spatial multiplexing gains through serving multiple users simultaneously [13], massive MIMO systems can enhance the system capacity significantly [13] and provide high spectral and energy efficiencies [13], [14], [16].

Typically, massive MIMO systems are launched in high attitude [13] and can be deployed using an array of antennas, which are either co-located at the same BS or distributed to cover a certain area [17]. Moreover, unlike the conventional approaches, where antennas are placed further away from each other to achieve spatial diversity, in practice, massive MIMO systems consider an antenna spacing of half-wavelength to maintain an implementable array aperture [13]. A noticeable feature of the massive MIMO system is that the effect of fast fading vanishes due to a large number of antennas deployed at the BS while serving multiple users [16].

However, massive MIMO systems face challenges from acquiring an accurate channel state information (CSI) at the BS because of channel estimation errors, feedback delays, and quantization errors [2], [13], [14]. Moreover, the feedback overhead in the uplink becomes prohibitive as the number of antennas grows without bound [2]. Furthermore, in addition to the synchronization issue [18], the limitation of space at the BS to pack a large number of antennas within a finite volume is another critical challenge of massive MIMO systems [2]. In this regard, to fully take advantage of the spatial multiplexing gain, high-frequency mmWave spectra can play a vital role due to the small wavelengths [2]. This causes massive MIMO systems in the mmWave band to suit ideally for addressing the high data rate and capacity demands in the fifth generation (5G) [19] and beyond systems by providing beamforming gain and supporting multiple data streams using general precoding schemes [20].

Since the massive MIMO improves the spectral efficiency by exploiting spatial multiplexing [21], combining the spatial multiplexing gain using the massive MIMO and the spectrum extension using the carrier aggregation technologies, massive data rates and network capacities can be obtained. In this regard, numerous studies have addressed the carrier aggregation in massive MIMO systems. For example, in [8], the authors have combined carrier aggregation technology with hybrid digital and analog beamforming architecture in massive MIMO systems and proposed a hybrid precoding algorithm to support aggregation of two carriers. Further, the authors in [22] have presented a novel sub-6 GHz and 28 GHz GaN switchable diplexer microwave monolithic integrated circuit (MMIC) for carrier aggregation with massive MIMO full-duplex link to mitigate self-interference in carrier aggregation operation and select antenna. Furthermore, in [23], the authors have introduced filter bank multicarrier as a potential candidate in the application of massive MIMO communication.

In spectrum trading, a certain portion of the licensed spectrum of one MNO can be leased by another MNO to increase its available spectrum. In this regard, the authors in [24] have considered spectrum trading in the context of multiple sellers and multiple buyers, whereas the authors in [25] have proposed a scheme for selling the spectra of multiple primary users to multiple secondary users. Likewise, the authors of [26] have proposed a matching based double auction mechanism for spectrum trading with differential privacy, whereas in [27], the authors have introduced a bandwidth-auction game for the spectrum trading problem of a cellular network.

Further, in spectrum sharing, an MNO can share with the licensed spectrum of another MNO using techniques such as cognitive radio by controlling the BS transmission power both opportunistically (e.g., interweave spectrum access) and simultaneously (e.g., underlay spectrum access) under mutual understanding between MNOs. In this aspect, the authors in [28] have proposed a technique to share both licensed and unlicensed spectra with small cells in 3-dimensional (3D) buildings to achieve high spectral and energy efficiencies. Also, in [29], the authors have proposed a technique to share the licensed spectrum of all MNOs in a country with in-building small cell BSs (SBSs) of each MNO. Further, the authors have studied the main concepts of dynamic spectrum sharing and different sharing scenarios in [30]. Furthermore, in [31], the authors have studied spectrum sharing approaches in mmWave systems.

However, in spectrum reusing, the same spectrum of an MNO can be reused to its BSs in space subject to satisfying a minimum co-channel interference (CCI) constraint. In this point, in [32], the authors have proposed an analytical model to reuse the microwave spectrum in [32] and the 28 GHz mmWave spectrum in [33] in a 3D building of SBSs. In [34], the authors have investigated a number of fractional frequency reuse (FFR) schemes, whereas, in [35], the authors have proposed dynamic fractional frequency reuse (DFFR) method for reducing the inter-cell interference automatically.

However, all these approaches aforementioned can be avoided if, instead of allocating a portion of the spectrum specified for a country, the countrywide full-spectrum is made available to each MNO for a certain license renewed term t_{rnw} such that each MNO in a country can access the full-spectrum dynamically subject to avoiding CCI. This results in overcoming the lack of required spectrum of an MNO because of the availability of the large countrywide full-spectrum to serve its user demand, as well as addressing the issue of the under-utilized or unused spectrum of an MNO by allowing dynamic access to the countrywide full-spectrum to improve its spectrum utilization, which, however, has not been addressed yet in the existing literature.

C. CONTRIBUTION

Hence, to increase the spectrum availability and utilization, in this paper, we present a new paradigm for the spectrum allocation called licensed countrywide full-spectrum allocation (LCFSA) to allocate the licensed countrywide full 28 GHz mmWave spectrum to each MNO of a country to operate its small cells per multistory building subject to avoiding CCI either in the time-domain or in the frequency-domain. Further, because of the low transmission power of an SBS and a high floor penetration loss, as well as internal-wall loss, experienced by a mmWave signal, the countrywide full mmWave spectrum of an MNO can be reused to its small cells within a building subject to satisfying a minimum CCI constraint set by the MNO itself. Likewise, due to a high external wall penetration loss of a building and the distance-dependent free-space path-loss between buildings, the countrywide full mmWave spectrum of an MNO can be reused to its small cells deployed in adjacent buildings as well. These results in improving further the utilization of the countrywide 28 GHz mmWave spectrum.

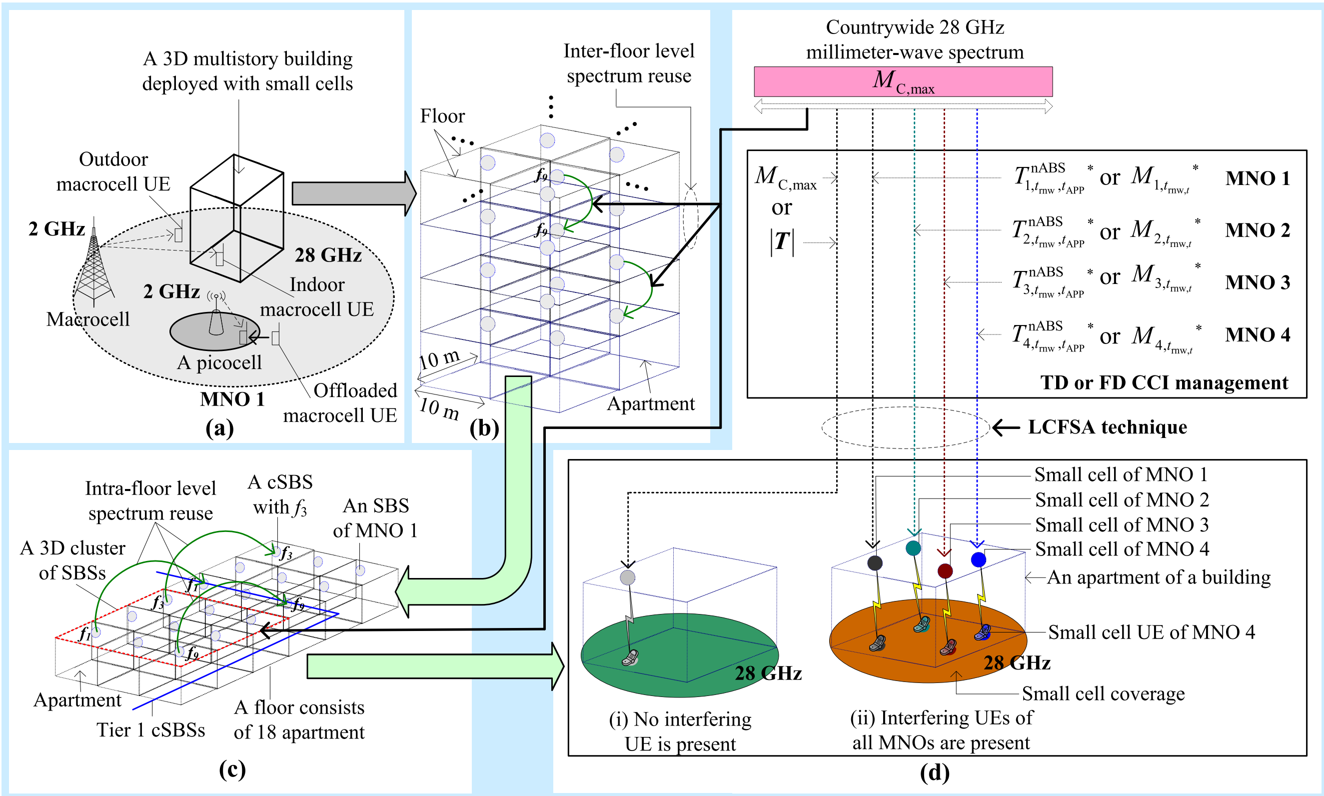

FIGURE 1. A system architecture consisting of four MNOs in a country. (a) the detailed architecture for MNO 1; (b) a 3D multistory building of small cells; (c) a floor of the multistory building consisting of 18 apartments; (d) an illustration for the application of the proposed technique both with the time-domain (TD) and frequency-domain (FD), CCI management schemes for (i) no existence of interfering UEs of other MNOs, as well as (ii) the existence of interfering UEs of all MNOs countrywide, with an SBS of MNO 1 in an apartment of a building.

D. ORGANIZATION

In addressing the proposed LCFSA technique, we present the system architecture and the proposed LCFSA technique in section II. Moreover, CCI avoidance schemes for each MNO in both the time-domain, as well as the frequency-domain, are presented and the conditions for optimality in each domain are defined. In section III, we derive average capacity, spectral efficiency (SE), energy efficiency (EE), and cost efficiency (CE) for the proposed LCFSA technique. In section IV, extensive numerical and simulation results and analyses for an example scenario of a country consisting of four MNOs are carried out for the existence of the maximum number of interfering UEs, as well as no interfering UEs, with an SBS of an MNO in an apartment of a building. Also, it is shown that the proposed LCFSA technique can satisfy the required SE and EE for sixth-generation (6G) mobile systems by changing either spectrum reuse factor (RF) or the number of buildings per macrocell, or both. We conclude the paper in section V.

II. SYSTEM ARCHITECTURE, PROPOSED TECHNIQUE, CCI MANAGEMENT AND SPECTRUM REUSE

A. SYSTEM ARCHITECTURE

Assume that four MNOs are operating countrywide, each having three types of BSs, namely macrocell BSs (MBSs), picocell BSs (PBSs), and SBSs. Due to considering a similar architecture for each MNO, only one MNO, particularly MNO 1, is detailed as shown in Fig.1. SBSs are deployed indoors (i.e., only within multistory buildings), one per apartment for each MNO. Buildings as well as PBSs are located throughout the coverage of each macrocell of MNO 1. Several macrocell UEs are considered indoors, as well as offloaded by PBSs outdoors. Except for getting offloaded by PBSs, both indoor and outdoor macrocell UEs are served by the MBS itself. Due to a small coverage and low transmission power of an SBS, we assume that an SBS of any MNO can serve only one UE at a time. Because of inherent favorable characteristics, both MBSs and PBSs are considered operating at a low-frequency 2 GHz microwave band to cover a large area outdoors, whereas SBSs are operating at a high-frequency 28 GHz mmWave band to cover a small area at a high data rate indoors.

Since user traffic demands of different MNOs in a country vary abruptly over time and space, the demand for the required amount of spectra for different MNOs also changes correspondingly. By exploiting such diversity in traffic demands of different MNOs countrywide, each of the four MNOs is given access to the countrywide full 28 GHz mmWave spectrum subject to avoiding CCI either in the time-domain or in the frequency-domain. In this regard, we consider employing the enhanced intercell interference coordination (eICIC) technique in both the time-domain and frequency-domain to allow respectively time-orthogonality and frequency-orthogonality to each MNO in accessing the full 28 GHz mmWave spectrum specified for a country. Since CCI for an SBS of MNO 1 in an apartment of a building changes with the presence of UEs of other MNOs, for simplicity, we show only the best-case (i.e., presence of no interfering UE), as well as the worst-case (i.e., presence of all interfering UEs), CCI scenarios for an SBS of MNO 1 in an apartment in Fig.1(d). In the following section, we propose a technique to allocate the countrywide full 28 GHz mmWave spectrum to each MNO in a country by presenting CCI management both in the time-domain, as well as frequency-domain.

B. PROPOSED LICENSED COUNTRYWIDE FULL-SPECTRUM ALLOCATION TECHNIQUE

We propose a novel licensed countrywide full-spectrum allocation (LCFSA) technique for mmWave (i.e., 28 GHz spectrum bands) mobile systems stated as follows. *Each MNO of a country is assigned with the countrywide full 28 GHz mmWave spectrum to operate its small cells deployed in each multistory building at the cost of paying the spectrum licensing fee subject to avoiding CCI. The allocated spectrum to each MNO can also be reused further to its small cells both within the same building, as well as adjacent buildings. The amount of the spectrum licensing fee for an MNO is updated corresponding to the change in its number of subscribers at each license renewed term* t_{rnw}.

Hence, unlike the traditional static licensed spectrum allocation (SLSA) technique (e.g., auction) where a dedicated portion of the licensed spectrum is allocated to an MNO for a long term without taking into account of any concern of its actual user demand, in the proposed LCFSA technique, each MNO is allocated to the countrywide full 28 GHz mmWave spectrum for a certain license renewed term t_{rnw} by the national regulatory agency (NRA) or any third-party subject to avoiding CCI. Hence, due to the availability of a large spectrum, an MNO can use as much spectrum as it needs to address its actual user demand at any renewed term. This results in overcoming the lack of a sufficient amount of spectrum of an MNO to serve its user demand, as well as addressing the issue of the under-utilized or unused spectrum of another MNO, such that the overall countrywide spectrum utilization is improved.

Further, in the proposed LCFSA technique, at the end of any term t_{rnw}, each MNO pays the spectrum licensing fee to the NRA based on its number of subscribers at t_{rnw} with respect to that of other MNOs countrywide. Hence, unlike bound to pay for the unused spectrum in the traditional SLSA technique, the proposed LCFSA technique allows an MNO to pay the licensing fee only for the amount of spectrum that it uses. Furthermore, because of a high floor penetration loss, as well as internal-wall loss, experienced by a mmWave signal, the countrywide full mmWave spectrum of an MNO can be reused to its small cells within a building subject to satisfying a minimum CCI constraint set by the MNO itself. Likewise, due to a high external wall penetration loss of a building and the distance-dependent free-space path-loss between buildings, the countrywide full mmWave spectrum of an MNO can be reused to its small cells deployed in adjacent buildings. This results in improving further the utilization of the countrywide 28 GHz mmWave spectrum.

C. CO-CHANNEL INTERFERENCE MANAGEMENT

Since all MNOs consider operating in-building small cells at the same countrywide full 28 GHz mmWave spectrum, CCI occurs when small cell UEs of more than one MNO are scheduled simultaneously. Such CCI can be avoided by allocating UEs orthogonally both in time-domain, as well as in frequency-domain, as given below.

1) TIME-DOMAIN CCI AVOIDANCE

In time-domain CCI avoidance, small cell UEs of different MNOs are allocated at a different time using techniques such as the almost blank subframe (ABS) based eICIC as shown in Fig.2(a). Assume that each small cell $s_{x,o}$ of an MNO o can serve the maximum of one UE $u_{x,o}$ at a time. Also, a UE of not more than one MNO o can be served at the same transmission time interval (TTI) over an ABS pattern period (APP) t_{APP} subject to satisfying the condition that if a UE of any MNO o exists within the coverage of a small cell of any other MNOs $\boldsymbol{O}\backslash o$, it must be scheduled to at least one TTI per APP to address fairness as shown in Fig.2(a). The number of TTIs allocated to a UE $u_{x,o}$ of an SBS $s_{x,o}$ of an MNO o is the number of non-ABSs per APP t_{APP}. This implies that the duration of an APP t_{APP} in terms of TTIs should be at least the number of MNOs of a country.

Hence, the number of non-ABSs per APP t_{APP} for an MNO to avoid CCI in time-domain can be stated as follows. The number of non-ABSs per APP t_{APP} allocated to a UE $u_{x,o}$ of $s_{x,o}$ of an MNO o is defined in accordance with the ratio of the number of subscribers $N_{o,t_{\text{rnw}}}$ of the MNO o at term t_{rnw} to the sum of the total number of subscribers of MNOs $\boldsymbol{O}\backslash o$ (including $N_{o,t_{\text{rnw}}}$) such that a UE $u_{x,\boldsymbol{O}\backslash o}$ corresponding to the MNO $\boldsymbol{O}\backslash o$ is present within the coverage of the small cell $s_{x,o}$ of the MNO o in any TTI of the previous APP $(t_{\text{APP}}-1)$ at term t_{rnw}. In this regard, using any conventional spectrum sensing technique, the presence of an interfering UE $u_{x,\boldsymbol{O}\backslash o}$ can be detected either by the small cell $s_{x,o}$ or by its small cell UE $u_{x,o}$.

Now, to find a generic expression for the optimal value of non-ABSs for an MNO $o \in \boldsymbol{O}$ at any APP t_{APP}, let O denote the maximum number of MNOs of a country such that $o \in \boldsymbol{O}$:$\boldsymbol{O} = \{1, 2, \ldots, O\}$. Let $s_{x,o} \in \boldsymbol{S_{x,o}} = \left\{0, 1, 2, 3, \ldots, S_{\text{F},o}\right\}$ denote the number of small cells of an MNO o deployed in any building $l \in \boldsymbol{L} = \{1, 2, 3, \ldots, L\}$. Let $u_{x,o} \in \boldsymbol{U_{x,o}} = \left\{0, 1, 2, 3, \ldots, U_{\text{F},o}\right\}$ denote the number of UEs of an MNO o corresponding to $s_{x,o} \in \boldsymbol{S_{x,o}}$ in any $l \in \boldsymbol{L}$. Let $M_{\text{C,max}}$ denote the countrywide total amount of mmWave spectrum defined in terms of the number of

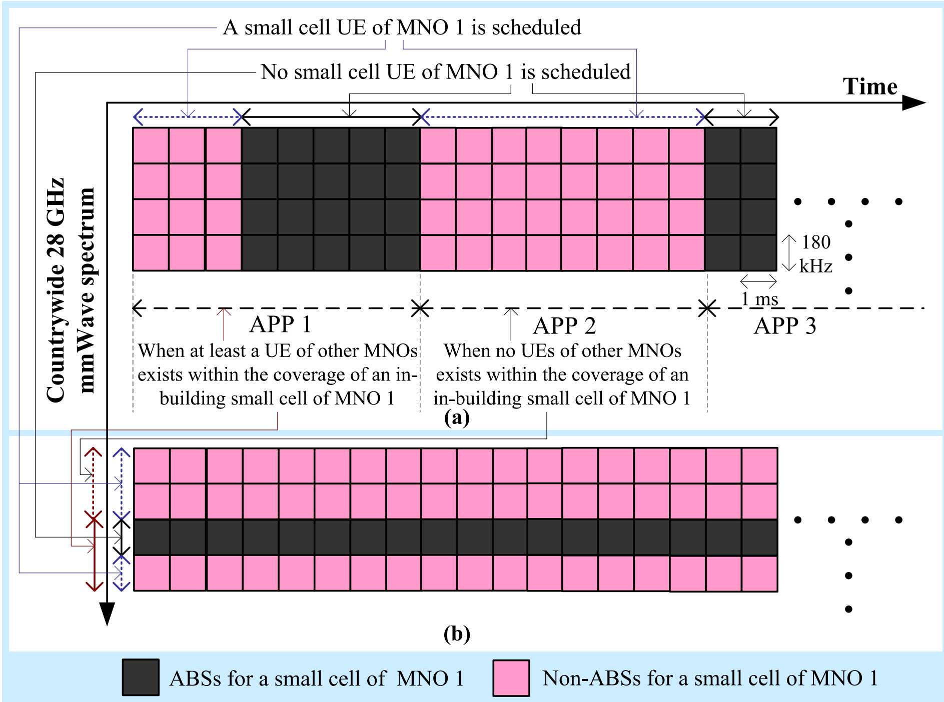

FIGURE 2. CCI avoidance techniques. (a) time-domain (b) frequency-domain.

resource blocks (RBs) where an RB is equal to 180 kHz. Let $N_{o,t_{\text{rnw}}}$ denote the total number of subscribers of an MNO o such that $\sum_o^O N_{o,t_{\text{rnw}}} \leq N_{\text{C, max},t_{\text{rnw}}}$ where $N_{\text{C, max},t_{\text{rnw}}}$ denotes the maximum number of subscribers of a country at t_{rnw}. Then, the optimal value of non-ABSs for an MNO $o \in \boldsymbol{O}$ at any APP t_{APP} can be found by solving the following problem.

$$\begin{aligned} &\min_{o\in\boldsymbol{O}} T^{\text{nABS}}_{o,t_{\text{rnw}},t_{\text{APP}}} \\ &\text{subject to (a) } N_{o,t_{\text{rnw}}}\Big/N_{t_{\text{rnw}},t_{\text{APP}}} = T^{\text{nABS}}_{o,t_{\text{rnw}},t_{\text{APP}}}\Big/T_{\text{APP}} \\ &\qquad\quad (b)\ \forall o \forall t_{\text{rnw}} \sum\nolimits_o^O N_{o,t_{\text{rnw}}} \leq N_{\text{C, max},t_{\text{rnw}}} \end{aligned} \tag{1}$$

The solution to the above optimization problem is given by (2), which is given in Proof 1.

$$T^{\text{nABS}}_{o,t_{\text{rnw}},t_{\text{APP}}}{}^{*} = \left\lceil\left(\left(N_{o,t_{\text{rnw}}}\Big/\sum_{o=1}^{O}(1_{\nu_o}(N_{o,t_{\text{rnw}}})\times N_{o,t_{\text{rnw}}})\right)\times T_{\text{APP}}\right)\right\rceil \tag{2}$$

Proof 1: The solution to the optimization problem in (1) can be found as follows. In general, the number of subscribers of all MNOs is not the same at any t_{rnw}. Hence, assume that $N_{1,t_{\text{rnw}}} > N_{2,t_{\text{rnw}}} > \ldots > N_{O,t_{\text{rnw}}}$ at t_{rnw} such that the constraint 1(b) is satisfied. Since a UE of any MNO $\boldsymbol{O}\backslash o$ in any TTI of an t_{APP} may not exist within a building l of small cells of an MNO o, $N_{t_{\text{rnw}},t_{\text{APP}}}$ can be expressed for $O = 4$ as as

$$N_{t_{\text{rnw}},t_{\text{APP}}} = \sum_{o=1}^{O}\left(1_{\nu_o}\left(N_{o,t_{\text{rnw}}}\right)\times N_{o,t_{\text{rnw}}}\right) \tag{3}$$

where $\nu_o \in \left\{N_{1,t_{\text{rnw}}}, N_{2,t_{\text{rnw}}} N_{3,t_{\text{rnw}}}, N_{4,t_{\text{rnw}}}\right\}$. $1(\cdot)$ defines that $1(\cdot) = 1$ if $N_{o,t_{\text{rnw}}}$ exists in the set ν_o; otherwise, $1(\cdot) = 0$.

Since the number of ABSs and non-ABSs is strictly an integer, using (3), as well as the constraint 1(a), the optimal value of $T^{\text{nABS}}_{o,t_{\text{rnw}},t_{\text{APP}}}$ is given by,

$$T^{\text{nABS}}_{o,t_{\text{rnw}},t_{\text{APP}}}{}^{*} = \left(\frac{N_{o,t_{\text{rnw}}}}{N_{t_{\text{rnw}},t_{\text{APP}}}}\right)\times T_{\text{APP}} : o \in \boldsymbol{O}$$

$$T^{\text{nABS}}_{o,t_{\text{rnw}},t_{\text{APP}}}{}^{*} = \left\lceil\left(\left(N_{o,t_{\text{rnw}}}\Big/\sum_{o=1}^{O}\left(1_{\nu_o}\left(N_{o,t_{\text{rnw}}}\right)\times N_{o,t_{\text{rnw}}}\right)\right)\times T_{\text{APP}}\right)\right\rceil$$

Hence, $T^{\text{ABS}}_{o,t_{\text{rnw}},t_{\text{APP}}}{}^{*} = \left(T_{\text{APP}} - T^{\text{nABS}}_{o,t_{\text{rnw}},t_{\text{APP}}}{}^{*}\right)$ ■

2) FREQUENCY-DOMAIN CCI AVOIDANCE

In frequency-domain CCI avoidance, UEs of all MNOs O are allocated orthogonally to different portions of the countrywide full 28 GHz mmWave spectrum as shown in Fig.2(b). Particularly, UEs of not more than one MNO can be allocated to the same frequency at any TTI per APP. Like time-domain CCI avoidance, the existence of an interfering UE can be detected either by the small cell or by its UE using any conventional spectrum sensing technique. Following the time-domain CCI avoidance, assume that the amount of spectrum allocated to a UE $u_{x,o}$ of $s_{x,o}$ of an MNO o is defined in accordance with the ratio of the number of subscribers $N_{o,t_{\text{rnw}}}$ of an MNO o at term t_{rnw} to the sum of the total number of subscribers of MNOs $\boldsymbol{O}\backslash o$ (including $N_{o,t_{\text{rnw}}}$) such that a UE $u_{x,\boldsymbol{O}\backslash o}$ corresponding to the MNO $\boldsymbol{O}\backslash o$ is present within the coverage of the small cell $s_{x,o}$ of the MNO o in each TTI at term t_{rnw} so long as $u_{x,\boldsymbol{O}\backslash o}$ exists. Then, the optimal amount of licensed 28 GHz spectrum $M_{o,t_{\text{rnw},t}}$ in RBs for an MNO o at a term t_{rnw} in any TTI t can be found by solving the following problem.

$$\begin{aligned}&\min_{o\in\boldsymbol{O}} M_{o,t_{\text{rnw},t}}\\&\text{subject to (a) } N_{o,t_{\text{rnw}}}/N_{t_{\text{rnw}},t} = M_{o,t_{\text{rnw},t}}/M_{\text{C, max}}\\&\qquad\text{(b) } \forall o \forall t_{\text{rnw}} \sum\nolimits_{o}^{O} N_{o,t_{\text{rnw}}} \le N_{\text{C, max},t_{\text{rnw}}}\end{aligned}\tag{4}$$

The solution to the above optimization problem is given by (5) and is given in Proof 2.

$$M_{o,t_{\text{rnw},t}}{}^{*} = \left(\left\lceil\left(N_{o,t_{\text{rnw}}}\Big/\sum_{o=1}^{O}\left(1_{\nu_o}\left(N_{o,t_{\text{rnw}}}\right)\times N_{o,t_{\text{rnw}}}\right)\right)\right\rceil\times M_{\text{C, max}}\right)\tag{5}$$

Proof 2: The solution of the above optimization problem can be found following the same process as in case of the time-domain CCI avoidance such that $N_{t_{\text{rnw}},t}$ can be expressed as

$$N_{t_{\text{rnw}},t} = \sum_{o=1}^{O}\left(1_{\nu_o}\left(N_{o,t_{\text{rnw}}}\right)\times N_{o,t_{\text{rnw}}}\right)\tag{6}$$

Now, using the constraint 4(a) and (6), the optimal value of $M_{o,t_{\text{rnw},t}}$ is given by,

$$M_{o,t_{\text{rnw},t}}{}^{*} = \left(\frac{N_{o,t_{\text{rnw}}}}{N_{t_{\text{rnw}},t}}\right)\times M_{\text{C, max}} : o\in\boldsymbol{O}$$

$$M_{o,t_{\text{rnw},t}}{}^{*} = \left(\left\lceil\left(N_{o,t_{\text{rnw}}}\Big/\sum_{o=1}^{O}\left(1_{\nu_o}\left(N_{o,t_{\text{rnw}}}\right)\times N_{o,t_{\text{rnw}}}\right)\right)\right\rceil\times M_{\text{C, max}}\right)$$

■

Note that in both the time-domain and frequency-domain, if a UE of any MNO $\boldsymbol{O}\backslash o$ in any TTI does not exist in the coverage of a small cell s_x of an MNO o in any building l, then $N_{t_{\text{rnw}},t_{\text{APP}}} = N_{o,t_{\text{rnw}}}$ in (3) and $N_{t_{\text{rnw}},t} = N_{o,t_{\text{rnw}}}$ in (6), which result in $T^{\text{nABS}}_{o,t_{\text{rnw}},t_{\text{APP}}}{}^{*} = T_{\text{APP}}$ and $M^{*}_{o,t_{\text{rnw},t}} = M_{\text{C, max}}$ respectively. Hence, the licensed countrywide full 28 GHz spectrum can be allocated in all TTIs to all UEs $u_{x,o} \in \boldsymbol{U_{x,o}}$ of all small cells $s_{x,o} \in \boldsymbol{S_{x,o}}$ of an MNO o in both the time-domain and frequency-domain CCI avoidance schemes. The same process described above applies to all MNOs $o \in \boldsymbol{O}$ at each renewed term t_{rnw} to update $T^{\text{nABS}}_{o,t_{\text{rnw}},t_{\text{APP}}}$ in the time-domain and $M_{o,t_{\text{rnw},t}}$ in the frequency-domain to avoid CCI such that the countrywide full 28 GHz mmWave spectrum can be allocated to all small cells of each MNO o at the cost of paying the licensing fee based on its number of subscribers $N_{o,t_{\text{rnw}}}$ at t_{rnw} with respect to that of other MNOs $\boldsymbol{O}\backslash o$ countrywide.

3) A CASE STUDY FOR THE APPLICATION OF LCFSA

Figure 3 shows the application of the proposed LCFSA technique with the frequency-domain CCI avoidance to allocate the countrywide full 28 GHz mmWave spectrum to all four MNOs $\boldsymbol{O} = \{1, 2, 3, 4\}$ in a country with the number of subscribers $N_{o,t_{\text{rnw}}}$ of 40%, 30%, 20%, and 10% of $N_{\text{C, max},t_{\text{rnw}}}$ respectively at any renewed term t_{rnw}. According to (5), the amount of spectrum allocated to an SBS of any MNO o in an apartment in any TTI t depends on the presence of UEs of other MNOs $\boldsymbol{O}\backslash o$. Since an SBS of any MNO o in an apartment of a building can serve only one UE at a time, the maximum number of four UEs (one from each MNO) can exist in an apartment. In this regard, a UE of an SBS for any MNO o can exist with other UEs of MNOs $\boldsymbol{O}\backslash o$ in a total of eight possible ways in an apartment. Figure 3 shows these eight possible ways of existence for a UE of an SBS of MNO 1 with that of MNOs 2, 3, and 4, and the corresponding countrywide full mmWave spectrum allocation to each MNO using (5).

The maximum amount of the countrywide full-spectrum is allocated to MNO 1 when no UE of $\boldsymbol{O}\backslash o = 1$ exists (i.e., $\boldsymbol{O} = \{1\}$) with that of MNO 1 in an apartment. Likewise, the minimum spectrum is allocated to MNO 1 when all UEs of $\boldsymbol{O}\backslash o = 1$ exist (i.e., $\boldsymbol{O} = \{1, 2, 3, 4\}$) in an apartment. In general, as the presence of the number of UEs of other MNOs $\boldsymbol{O}\backslash o = 1$ with that of MNO 1 in an apartment increases, the allocation of spectrum to MNO 1 decreases, and vice versa. The same explanation applies to the proposed LCFSA technique with the time-domain CCI avoidance such that instead of the spectrum, the amount of time in terms of TTIs per APP is allocated to an SBS of any MNO o in an apartment to use the countrywide full-spectrum based on the presence of UEs of other MNOs $\boldsymbol{O}\backslash o$ as given by (2).

D. 28 GHz MILLIMETER-WAVE SPECTRUM REUSE

High-frequency mmWave signals experience high attenuation effects in indoor environments due to a high distance-dependent path loss, floor penetration loss, as well as internal-wall loss within a multistory building. Further, the transmission power of an in-building SBS is low. Because of these high losses of mmWave signals, as well as low transmission power of an SBS, within a building, the 28 GHz mmWave spectrum can be reused to small cells within a building more than once subject to satisfying a minimum CCI constraint from one co-channel SBS (cSBS) to another operating at the same reused spectrum. A minimum distance between cSBSs both in the intra-floor level, as well as inter-floor level, corresponding to the respective CCI constraint, can be defined. The set of SBSs defined by these minimum distances in the intra-and inter-floor levels forms a 3D cluster of SBSs such that the same countrywide full 28 GHz mmWave spectrum for an MNO can be reused to each 3D cluster of SBSs, resulting in reusing the same spectrum more than once to small cells in a building (i.e., intra-building level). We adopt the model proposed by the author in [33] for

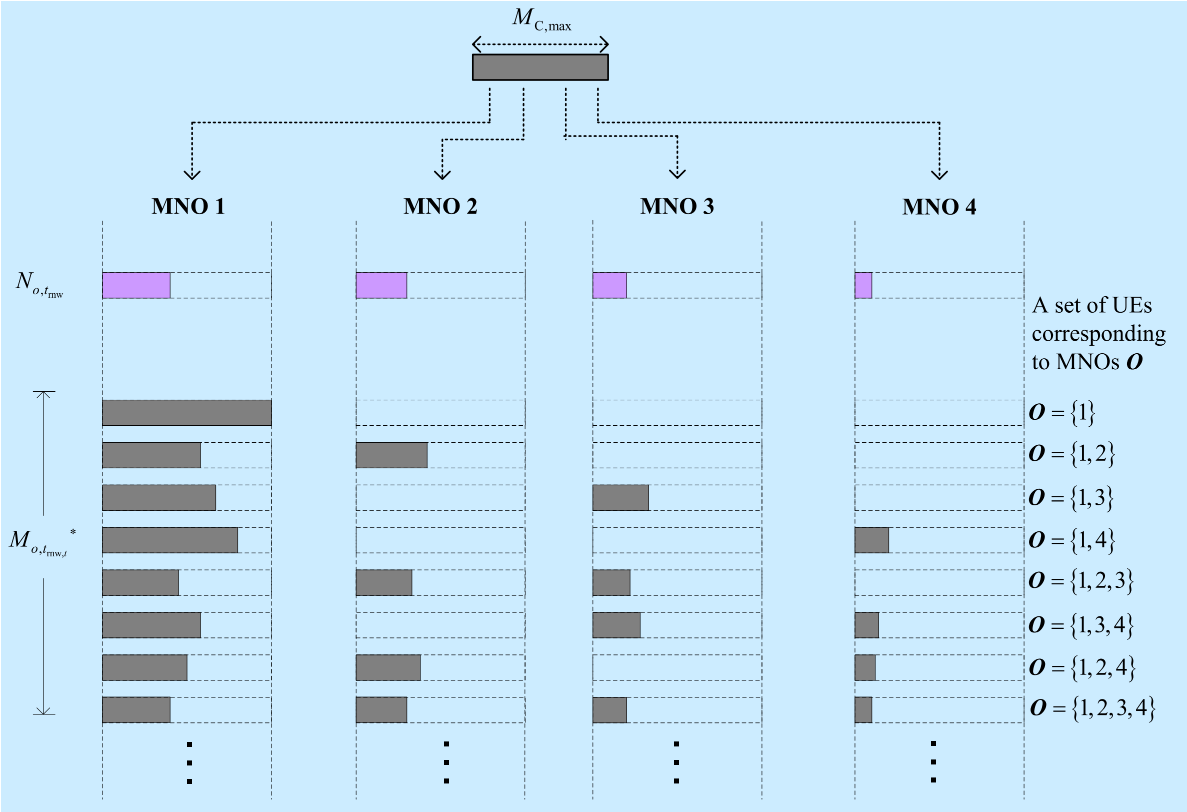

FIGURE 3. **An illustration for the application of the proposed LCFSA technique with frequency-domain CCI avoidance to allocate the countrywide full 28 GHz mmWave spectrum to all four MNOs $\boldsymbol{O} = \{1, 2, 3, 4\}$ in a country at any renewed term t_{rnw} with the variation of the number of UEs of MNOs present in an apartment of a building with respect to the SBS of MNO 1.**

the 28 GHz mmWave spectrum to define a 3D cluster of small cells in a multistory building, which we present in brief in the following.

The minimum distance between cSBSs operating at the 28 GHz mmWave spectrum in the intra-floor level and inter-floor level for an MNO o can be given respectively by,

$$d_{\mathrm{tra},o}{}^* = d_\mathrm{m} \times \left(\frac{\lambda_{\mathrm{tra},o}}{I_{\mathrm{tra},o}}\right)^{1.797^{-1}} \tag{7}$$

$$d_{\mathrm{ter},o}{}^* \geq d_\mathrm{m} \times \left(\frac{\left(\frac{\lambda_{\mathrm{ter},o}}{I_{\mathrm{ter},o}}\right)}{10^{\frac{\alpha_\mathrm{f}(d_{\mathrm{ter},o})}{10}}}\right)^{1.797^{-1}} \tag{8}$$

where d_m denotes the minimum distance between a cSBS and a small cell UE for all MNOs. $\lambda_{\mathrm{tra},o}$ and $\lambda_{\mathrm{ter},o}$ denote respectively the maximum number of cSBSs for an MNO o in the intra-floor and inter-floor levels in a building. Likewise, $I_{\mathrm{tra},o}$ and $I_{\mathrm{ter},o}$ denote respectively the optimal value of CCI for an MNO o in the intra-floor and inter-floor levels. $\alpha_\mathrm{f}\left(d_{\mathrm{ter},o}\right)$ denotes the floor penetration loss at 28 GHz for an MNO o. The path loss model for the 28 GHz mmWave for the distance d considered to derive the above equations is given by,

$$\mathrm{PL}\,(\mathrm{dB}) = 61.38 + 17.97 \log_{10}(d) + X \tag{9}$$

where X denotes the Gaussian random variable that represents the shadowing effect of the 28 GHz mmWave signal.

Recall that the set of SBSs defined by these minimum distances $d_{\mathrm{tra},o}{}^*$ and $d_{\mathrm{ter},o}{}^*$ for an MNO o forms a 3D cluster of SBSs in a building. Hence, let $\lambda_{\mathrm{cl,tra},o}$ and $\lambda_{\mathrm{cl,ter},o}$ denote respectively the number of SBSs corresponding to $d_{\mathrm{tra},o}{}^*$ in the intra-floor level and $d_{\mathrm{ter},o}{}^*$ in the inter-floor level, which can be expressed as follows.

$$\lambda_{\mathrm{cl,tra},o} = \left(\mathrm{ceil}\left(\frac{\left(d_{\mathrm{tra},o}{}^* + (0.5 \times a)\right)}{a}\right)\right)^2 \tag{10}$$

$$\lambda_{\mathrm{cl,ter},o} = \mathrm{ceil}\left(\frac{d_{\mathrm{ter},o}{}^*}{d_\mathrm{f}}\right) \tag{11}$$

where a denotes the side length of 10 m of a square apartment and d_f denotes the height of a floor. Hence, the size of a 3D cluster of SBSs $\lambda_{\mathrm{cl,3D},o}$ and the corresponding 28 GHz mmWave spectrum RF ε_o in a building for an MNO o are given respectively by,

$$\lambda_{\mathrm{cl,3D},o} = \left(\lambda_{\mathrm{cl,tra},o} \times \lambda_{\mathrm{cl,ter},o}\right) \tag{12}$$

$$\varepsilon_o = \frac{S_\mathrm{F}}{\lambda_{\mathrm{cl,3D},o}} \tag{13}$$

where S_F denotes the number of small cells in a building. Hence, the same countrywide full 28 GHz mmWave spectrum for an MNO o can be reused to each $\lambda_{\text{cl,3D},o}$ such that the same countrywide full 28 GHz mmWave spectrum can be reused more than once (defined by ε_o) to small cells S_F in a building. Detailed modeling for the 3D clustering of SBSs in a building for the 28 GHz mmWave spectrum described above is out of the scope of this paper, which can be found in [33].

Likewise, due to experiencing a high external wall penetration loss of a building and distant-dependent free-space path loss between adjacent buildings, the countrywide full 28 GHz mmWave spectrum of an MNO can be reused to its small cells deployed in adjacent buildings, resulting in reusing the same spectrum in the inter-building level. Hence, in addition to increasing the amount of available 28 GHz mmWave spectrum for an MNO by allocating the countrywide full 28 GHz mmWave spectrum subject to avoiding CCI either in the time-domain or the frequency-domain described above, the countrywide full 28 GHz mmWave spectrum can also be reused multiple times to small cells of an MNO located both within the same building (limited by the number of apartments per building), as well as adjacent buildings (limited by the number multistory buildings per macrocell).

III. MATHEMATICAL ANALYSIS

A. PRELIMINARIES

Assume that CCI constraints $I_{\text{tra},o}$ and $I_{\text{ter},o}$ for each MNO in a country are the same such that the size of a 3D cluster of SBSs $\lambda_{\text{cl,3D},o}$ for each MNO is the same, i.e. $\forall o\ \lambda_{\text{cl,3D},o} = \lambda_{\text{cl,3D}}$. Also, consider that the number of SBSs per multistory building for each MNO $S_{\text{F},o}$ is the same, i.e. $\forall o\ S_{\text{F},o} = S_\text{F}$. Then, the spectrum RF ε_o for each MNO in a building is also the same, i.e. $\forall o\ \ \varepsilon_o = \varepsilon$. Let $S_{\text{M},o}$ and $S_{\text{P},o}$ denote respectively the number of MBSs and the number of PBSs per MBS of an MNO o. Let, also, $\boldsymbol{T}$ denote simulation run time with the maximum time of Q (in time step each lasting 1 ms) such that $\boldsymbol{T} = \{1, 2, 3, \ldots, Q\}$. Assume that P_MC, P_PC, and P_SC denote respectively the transmission power of an MBS, a PBS, and an SBS of each MNO countrywide. Using Shannon's capacity formula, a link throughput at RB $= i$ in TTI $= t$ for an MNO o at a renewed term t_rnw in bps per Hz is given by [36], [37], (14), as shown at the bottom of the next page. where β denotes the implementation loss factor.

Let $M_{\text{MBS},o}$ denote the 2 GHz spectrum in RBs of a macrocell for an MNO o. Then, the total capacity of all macrocell UEs for an MNO o at t_rnw can be expressed as

$$\sigma_{\text{MBS},o}^{t_\text{rnw}} = \sum_{t=1}^{Q} \sum_{i=1}^{M_{\text{MBS},o}} \sigma_{t,i,o}^{t_\text{rnw}}\left(\rho_{t,i,o}^{t_\text{rnw}}\right) \tag{15}$$

where σ and ρ are responses over $M_{\text{MBS},o}$ RBs of all macro UEs in $t \in \boldsymbol{T}$ for an MNO o at t_rnw.

Now, let κ_C denote the cost of the total amount of mmWave spectrum $M_\text{C,max}$ allocated to a country. Recall that an MNO o pays the spectrum licensing fee based on its number of subscribers at t_rnw with respect to that of all MNOs countrywide $N_{\text{C, max},t_\text{rnw}}$. Let an MNO o pays κ_o corresponding to its subscribers N_{o,t_rnw} at term t_rnw such that κ_o and κ_C can be expressed as

$$\kappa_o = \kappa_\text{C} \times \left(\frac{N_{o,t_\text{rnw}}}{N_{\text{C, max},t_\text{rnw}}}\right) \tag{16}$$

$$\kappa_\text{C} = \sum_{o=1}^{O} \kappa_o \tag{17}$$

where $\sum_o^O N_{o,t_\text{rnw}} \leq N_{\text{C, max},t_\text{rnw}}$.

B. PROPOSED LCFSA WITH TIME-DOMAIN CCI AVOIDANCE

Let $\boldsymbol{T}_{o,t_\text{rnw},t_\text{APP}}^{\text{nABS}}$ denote a set including all non-ABSs $T_{o,t_\text{rnw},t_\text{APP}}^{\text{nABS}*}$ for an MNO $o \in \boldsymbol{O}$ at all APPs in $\boldsymbol{T}$ for a building l such that $\boldsymbol{T}_{o,t_\text{rnw},t_\text{APP}}^{\text{nABS}} \subseteq \boldsymbol{T}$. Let $t_{\text{ABS},o}$ and $t_{\text{nABS},o}$ denote respectively an ABS and a non-ABS over any APP t_APP for an MNO o such that $t_{\text{ABS},o} \in \boldsymbol{T}_{o,t_\text{rnw},t_\text{APP}}^{\text{ABS}}$ and $t_{\text{nABS},o} \in \boldsymbol{T}_{o,t_\text{rnw},t_\text{APP}}^{\text{nABS}} = \boldsymbol{T} \backslash \boldsymbol{T}_{o,t_\text{rnw},t_\text{APP}}^{\text{ABS}}$. If all SBSs of an MNO o in each multistory building l serves simultaneously in $t_{\text{nABS},o} \in \boldsymbol{T}_{o,t_\text{rnw},t_\text{APP}}^{\text{nABS}}$, then, the aggregate capacity served by an SBS and all SBSs per 3D cluster in a building (i.e., for $l = 1$) of an MNO o at a renewed term t_rnw when applying the proposed LCFSA technique with the time-domain CCI avoidance are given respectively by,

$$\sigma_{\text{TD},o,l=1,s_{x,o}}^{t_\text{rnw}} = \sum_{t=t_{\text{nABS},o} \in \boldsymbol{T}_{o,t_\text{rnw},t_\text{APP}}^{\text{nABS}}} \sum_{i=1}^{M_\text{C,max}} \sigma_{t,i,o}^{t_\text{rnw}}\left(\rho_{t,i,o}^{t_\text{rnw}}\right) \tag{18}$$

$$\sigma_{\text{TD},o,l=1,\lambda_\text{cl,3D}}^{t_\text{rnw}} = \sum_{s_{x,o}=1}^{\lambda_\text{cl,3D}} \sum_{t=t_{\text{nABS},o} \in \boldsymbol{T}_{o,t_\text{rnw},t_\text{APP}}^{\text{nABS}}} \sum_{i=1}^{M_\text{C,max}} \sigma_{t,i,o}^{t_\text{rnw}}\left(\rho_{t,i,o}^{t_\text{rnw}}\right) \tag{19}$$

Hence, the aggregate capacity served by all SBSs in a building of an MNO o at a renewed term t_rnw is given by,

$$\sigma_{\text{TD},o,l=1,S_{\text{F},o}}^{t_\text{rnw}} = \left(\varepsilon \times \sigma_{\text{TD},o,l=1,\lambda_\text{cl,3D}}^{t_\text{rnw}}\right)$$

The distance between an SBS and its serving small cell UE is short and the transmission power of an SBS is low. Moreover, a mmWave signal typically gets highly attenuated indoors, resulting in a small coverage of an SBS. Hence, taking all these into account, we assume a similar indoor signal propagation characteristics for all L buildings per macrocell for an MNO o at t_rnw. Then, by linear approximation, the system-level average capacity, SE, and EE for all MNOs O countrywide at t_rnw can be given respectively as follows for $l = L$,

$$\begin{aligned}
&\sigma_{\text{TD,cap},O}^{\text{sys},t_\text{rnw}}(L) \\
&= \sum_{o=1}^{O}\left(\sigma_{\text{MBS},o}^{t_\text{rnw}} + \left(L \times \sigma_{\text{TD},o,l=1,S_{\text{F},o}}^{t_\text{rnw}}\right)\right) \\
&\sigma_{\text{TD,cap},O}^{\text{sys},t_\text{rnw}}(L) \\
&= \sum_{o=1}^{O}\left(\sigma_{\text{MBS},o}^{t_\text{rnw}} + \left(L \times \varepsilon \times \sigma_{\text{TD},o,l=1,\lambda_\text{cl,3D}}^{t_\text{rnw}}\right)\right) \\
&\sigma_{\text{TD,SE},O}^{\text{sys},t_\text{rnw}}(L)
\end{aligned} \tag{20}$$

$$= \frac{\sum_{o=1}^{O}\left(\sigma_{\mathrm{MBS},o}^{t_{\mathrm{rnw}}} + \left(L \times \varepsilon \times \sigma_{\mathrm{TD},o,l=1,\lambda_{\mathrm{cl,3D}}}^{t_{\mathrm{rnw}}}\right)\right)}{\left(\left(M_{\mathrm{C,max}} + \sum_{o=1}^{O} M_{\mathrm{MBS},o}\right) \times Q\right)} \quad (21)$$

$$\sigma_{\mathrm{TD,EE},O}^{\mathrm{sys},t_{\mathrm{rnw}}}(L) = \frac{\sum_{o=1}^{O}\left((L \times S_{\mathrm{F},o} \times P_{\mathrm{SC}}) + (S_{\mathrm{P},o} \times P_{\mathrm{PC}}) + (S_{\mathrm{M},o} \times P_{\mathrm{MC}})\right)}{\left(\sum_{o=1}^{O}\left(\sigma_{\mathrm{MBS},o}^{t_{\mathrm{rnw}}} + \left(L \times \varepsilon \times \sigma_{\mathrm{TD},o,l=1,\lambda_{\mathrm{cl,3D}}}^{t_{\mathrm{rnw}}}\right)\right)\right)/Q} \quad (22)$$

Now, define cost efficiency (CE) as the cost required per unit achievable average capacity (i.e., per bps) such that the CE of small cell networks at term t_{rnw} can be expressed as follows.

$$\varsigma_{\mathrm{TD,CE},O}^{\mathrm{sys},t_{\mathrm{rnw}}} = \frac{\kappa_{\mathrm{C}}}{\sum_{o=1}^{O}\left(\sigma_{\mathrm{MBS},o}^{t_{\mathrm{rnw}}} + \left(L \times \varepsilon \times \sigma_{\mathrm{TD},o,l=1,\lambda_{\mathrm{cl,3D}}}^{t_{\mathrm{rnw}}}\right)\right)} \quad (23)$$

C. PROPOSED LCFSA WITH FREQUENCY-DOMAIN CCI AVOIDANCE

Like in the time-domain CCI avoidance, assume that all SBSs of an MNO o in each multistory building l serve simultaneously in all TTI $t \in \boldsymbol{T}$. Then, the aggregate capacity served by an SBS and all SBSs per 3D cluster in a building of an MNO o at a renewed term t_{rnw} when applying the proposed LCFSA technique with the frequency-domain CCI avoidance are given respectively by,

$$\sigma_{\mathrm{FD},o,l=1,s_{x,o}}^{t_{\mathrm{rnw}}} = \sum_{t \in \boldsymbol{T}} \sum_{i=1}^{M_{o,t_{\mathrm{rnw}},t}{}^{*}} \sigma_{t,i,o}^{t_{\mathrm{rnw}}}\left(\rho_{t,i,o}^{t_{\mathrm{rnw}}}\right) \quad (24)$$

$$\sigma_{\mathrm{FD},o,l=1,\lambda_{\mathrm{cl,3D}}}^{t_{\mathrm{rnw}}} = \sum_{s_{x,o}=1}^{\lambda_{\mathrm{cl,3D}}} \sum_{t \in \boldsymbol{T}} \sum_{i=1}^{M_{o,t_{\mathrm{rnw}},t}{}^{*}} \sigma_{t,i,o}^{t_{\mathrm{rnw}}}\left(\rho_{t,i,o}^{t_{\mathrm{rnw}}}\right) \quad (25)$$

Hence, the aggregate capacity served by all SBSs in a building of an MNO o at a renewed term t_{rnw} is given by,

$$\sigma_{\mathrm{FD},o,l=1,S_{\mathrm{F},o}}^{t_{\mathrm{rnw}}} = \left(\varepsilon \times \sigma_{\mathrm{FD},o,l=1,\lambda_{\mathrm{cl,3D}}}^{t_{\mathrm{rnw}}}\right) \quad (26)$$

Similarly, the system-level average capacity, SE, EE, and CE for all MNOs O countrywide at t_{rnw} can be expressed as follows for $l = L$,

$$\sigma_{\mathrm{FD,cap},O}^{\mathrm{sys},t_{\mathrm{rnw}}}(L) = \sum_{o=1}^{O}\left(\sigma_{\mathrm{MBS},o}^{t_{\mathrm{rnw}}} + \left(L \times \sigma_{\mathrm{FD},o,l=1,S_{\mathrm{F},o}}^{t_{\mathrm{rnw}}}\right)\right) \quad (27)$$

$$\sigma_{\mathrm{FD,cap},O}^{\mathrm{sys},t_{\mathrm{rnw}}}(L) = \sum_{o=1}^{O}\left(\sigma_{\mathrm{MBS},o}^{t_{\mathrm{rnw}}} + \left(L \times \varepsilon \times \sigma_{\mathrm{FD},o,l=1,\lambda_{\mathrm{cl,3D}}}^{t_{\mathrm{rnw}}}\right)\right)$$

$$\sigma_{\mathrm{FD,SE},O}^{\mathrm{sys},t_{\mathrm{rnw}}}(L) = \frac{\sum_{o=1}^{O}\left(\sigma_{\mathrm{MBS},o}^{t_{\mathrm{rnw}}} + \left(L \times \varepsilon \times \sigma_{\mathrm{FD},o,l=1,\lambda_{\mathrm{cl,3D}}}^{t_{\mathrm{rnw}}}\right)\right)}{\left(\left(M_{\mathrm{C,max}} + \sum_{o=1}^{O} M_{\mathrm{MBS},o}\right) \times Q\right)} \quad (28)$$

$$\sigma_{\mathrm{FD,EE},O}^{\mathrm{sys},t_{\mathrm{rnw}}}(L) = \frac{\sum_{o=1}^{O}\left((L \times S_{\mathrm{F},o} \times P_{\mathrm{SC}}) + (S_{\mathrm{P},o} \times P_{\mathrm{PC}}) + (S_{\mathrm{M},o} \times P_{\mathrm{MC}})\right)}{\left(\sum_{o=1}^{O}\left(\sigma_{\mathrm{MBS},o}^{t_{\mathrm{rnw}}} + \left(L \times \varepsilon \times \sigma_{\mathrm{FD},o,l=1,\lambda_{\mathrm{cl,3D}}}^{t_{\mathrm{rnw}}}\right)\right)\right)/Q} \quad (29)$$

$$\varsigma_{\mathrm{FD,CE},O}^{\mathrm{sys},t_{\mathrm{rnw}}} = \frac{\kappa_{\mathrm{C}}}{\sum_{o=1}^{O}\left(\sigma_{\mathrm{MBS},o}^{t_{\mathrm{rnw}}} + \left(L \times \varepsilon \times \sigma_{\mathrm{FD},o,l=1,\lambda_{\mathrm{cl,3D}}}^{t_{\mathrm{rnw}}}\right)\right)} \quad (30)$$

D. TRADITIONAL SLSA

Assume that in the traditional SLSA technique, each MNO is licensed exclusively for an equal amount of mmWave spectrum of M RBs. Then, the aggregate capacity served by an SBS, SBSs per 3D cluster, and all SBSs per building $l = 1$ of an MNO o at a renewed term t_{rnw} when applying the traditional SLSA technique are given respectively by,

$$\sigma_{\mathrm{SLSA},o,l=1,s_{x,o}}^{t_{\mathrm{rnw}}} = \sum_{t \in \boldsymbol{T}} \sum_{i=1}^{M} \sigma_{t,i,o}^{t_{\mathrm{rnw}}}\left(\rho_{t,i,o}^{t_{\mathrm{rnw}}}\right) \quad (31)$$

$$\sigma_{\mathrm{SLSA},o,l=1,\lambda_{\mathrm{cl,3D}}}^{t_{\mathrm{rnw}}} = \sum_{s_{x,o}=1}^{\lambda_{\mathrm{cl,3D}}} \sum_{t \in \boldsymbol{T}} \sum_{i=1}^{M} \sigma_{t,i,o}^{t_{\mathrm{rnw}}}\left(\rho_{t,i,o}^{t_{\mathrm{rnw}}}\right) \quad (32)$$

$$\sigma_{\mathrm{SLSA},o,l=1,S_{\mathrm{F},o}}^{t_{\mathrm{rnw}}} = \left(\varepsilon \times \sigma_{\mathrm{SLSA},o,l=1,\lambda_{\mathrm{cl,3D}}}^{t_{\mathrm{rnw}}}\right) \quad (33)$$

Then, the system-level average aggregate capacity, SE, EE, and CE for all MNOs O countrywide at t_{rnw} can be expressed as follows for $l = L$,

$$\sigma_{\mathrm{SLSA,cap},O}^{\mathrm{sys},t_{\mathrm{rnw}}}(L) = \sum_{o=1}^{O}\left(\sigma_{\mathrm{MBS},o}^{t_{\mathrm{rnw}}} + \left(L \times \sigma_{\mathrm{SLSA},o,l=1,S_{\mathrm{F},o}}^{t_{\mathrm{rnw}}}\right)\right) \quad (34)$$

$$\sigma_{\mathrm{SLSA,cap},O}^{\mathrm{sys},t_{\mathrm{rnw}}}(L) = \sum_{o=1}^{O}\left(\sigma_{\mathrm{MBS},o}^{t_{\mathrm{rnw}}} + \left(L \times \varepsilon \times \sigma_{\mathrm{SLSA},o,l=1,\lambda_{\mathrm{cl,3D}}}^{t_{\mathrm{rnw}}}\right)\right)$$

$$\sigma_{\mathrm{SLSA,SE},O}^{\mathrm{sys},t_{\mathrm{rnw}}}(L) = \frac{\sum_{o=1}^{O}\left(\sigma_{\mathrm{MBS},o}^{t_{\mathrm{rnw}}} + \left(L \times \varepsilon \times \sigma_{\mathrm{SLSA},o,l=1,\lambda_{\mathrm{cl,3D}}}^{t_{\mathrm{rnw}}}\right)\right)}{\left(\left(M_{\mathrm{C,max}} + \sum_{o=1}^{O} M_{\mathrm{MBS},o}\right) \times Q\right)} \quad (35)$$

$$\sigma_{t,i,o}^{t_{\mathrm{rnw}}}\left(\rho_{t,i,o}^{t_{\mathrm{rnw}}}\right) = \begin{cases} 0, & \rho_{t,i,o}^{t_{\mathrm{rnw}}} < -10\ \mathrm{dB} \\ \beta \log_2\left(1 + 10^{\left(\rho_{t,i,o}^{t_{\mathrm{rnw}}}(\mathrm{dB})/10\right)}\right), & -10\ \mathrm{dB} \le \rho_{t,i,o}^{t_{\mathrm{rnw}}} \le 22\ \mathrm{dB} \\ 4.4, & \rho_{t,i,o}^{t_{\mathrm{rnw}}} > 22\ \mathrm{dB} \end{cases} \quad (14)$$

TABLE 1. Simulation parameters and assumptions.

Parameters and Assumptions	Value
Countrywide perspective	
Total 28 GHz spectrum	200 MHz
Total number of MNOs and subscribers	4 and $N_{C,max}$
2 GHz spectrum per MNO	10 MHz
Number of subscribers for MNOs 1, 2, 3, and 4 respectively	40%, 30%, 20%, and 10% of $N_{C,max}$
For each MNO	
E-UTRA simulation case[1]	3GPP case 3
Cellular layout[2], inter-site distance (ISD)[1,2], transmission direction	Hexagonal grid, dense urban, 3 sectors per macrocell site, 1732 m, downlink
Carrier frequency[2,5]	2 GHz non-LOS (NLOS) for macrocells and picocells, 28 GHz LOS for all small cells
Number of cells	1 macrocell, 2 picocells, 90 small cells per building
Total BS transmission power[1] (dBm)	46 for macrocell[1,4], 37 for picocells[1], 19 for small cells[1,3,4]
Co-channel small-scale fading model[1,3,5]	Frequency selective Rayleigh for 2 GHz NLOS, none for 28 GHz LOS
Path loss — MBS and a UE[1] — Outdoor macrocell UE	PL(dB)=15.3 + 37.6 $\log_{10}R$, R is in m
Path loss — MBS and a UE[1] — Indoor macrocell UE	PL(dB)=15.3 + 37.6 $\log_{10}R + L_{ow}$, R is in m and L_{ow}=20 dB
Path loss — PBS and a UE[1]	PL(dB)=140.7+36.7 $\log_{10}R$, R is in km
Path loss — SBS and a UE[1,2,5]	PL(dB)=61.38+17.97 $\log_{10}R$, R is in m
Lognormal shadowing standard deviation (dB)	8 for MBS[2], 10 for PBS[1], and 9.9 for SBS[2,5]
Antenna configuration	Single-input single-output for all BSs and UEs
Antenna pattern (horizontal)	Directional (120^0) for MBS[1], omnidirectional for PBS[1] and SBS[1]
Antenna gain plus connector loss (dBi)	14 for MBS[2], 5 for PBS[1], 5 for SBS[1,3]
UE antenna gain[2,3]; Indoor macrocell UE[1]	0 dBi (for 2 GHz), 5 dBi (for 28 GHz, Biconical horn); 35%
UE noise figure[2,3] and UE speed[1]	9 dB (for 2 GHz) and 10 dB (for 28 GHz), 3 km/hr
Picocell coverage, the total number of macrocell UEs, and macrocell UEs offloaded to all picocells[1]	40 m (radius), 30, 2/15
3D multistory building and SBS models (square-grid apartments) — Number of buildings	L
3D multistory building and SBS models (square-grid apartments) — Number of floors per building	5
3D multistory building and SBS models (square-grid apartments) — Number of apartments per floor	18
3D multistory building and SBS models (square-grid apartments) — Number of SBSs per apartment	1
3D multistory building and SBS models (square-grid apartments) — Area of an apartment	10×10 m^2
Scheduler and traffic model[2]	Proportional Fair and full buffer
Type of SBSs	Closed Subscriber Group femtocell BSs
TTI[1] and scheduler time constant (t_c)	1 ms and 100 ms
Total simulation run time	8 ms

taken [1]from [39], [2]from [40], [3]from [41], [4]from [15], from [5][42].

$$\sigma^{sys,t_{rnw}}_{SLSA,EE,O}(L) = \frac{\sum_{o=1}^{O}\left(\left(L\times S_{F,o}\times P_{SC}\right)+\left(S_{P,o}\times P_{PC}\right)+\left(S_{M,o}\times P_{MC}\right)\right)}{\left(\sum_{o=1}^{O}\left(\sigma^{t_{rnw}}_{MBS,o}+\left(L\times\varepsilon\times\sigma^{t_{rnw}}_{SLSA,o,l=1,\lambda_{cl,3D}}\right)\right)\right)\Big/Q} \quad (36)$$

$$\varsigma^{sys,t_{rnw}}_{SLSA,CE,O} = \frac{\kappa_C}{\sum_{o=1}^{O}\left(\sigma^{t_{rnw}}_{MBS,o}+\left(L\times\varepsilon\times\sigma^{t_{rnw}}_{SLSA,o,l=1,\lambda_{cl,3D}}\right)\right)} \quad (37)$$

E. PERFORMANCE METRICS IMPROVEMENT FACTOR

Hence, the factor representing an improvement in average capacity, SE, EE, and CE can be expressed respectively for all MNOs O countrywide when applying the proposed LCFSA technique with the time-domain CCI avoidance as follows.

$$\varsigma^{sys,t_{rnw}}_{cap,TD,IF} = \frac{\sigma^{sys,t_{rnw}}_{TD,cap,O}(L)}{\sigma^{sys,t_{rnw}}_{SLSA,cap,O}(L)} \quad (38)$$

$$\varsigma^{sys,t_{rnw}}_{SE,TD,IF} = \frac{\sigma^{sys,t_{rnw}}_{TD,SE,O}(L)}{\sigma^{sys,t_{rnw}}_{SLSA,SE,O}(L)} \quad (39)$$

$$\varsigma^{sys,t_{rnw}}_{EE,TD,IF} = \frac{\sigma^{sys,t_{rnw}}_{TD,EE,O}(L)}{\sigma^{sys,t_{rnw}}_{SLSA,EE,O}(L)} \quad (40)$$

$$\varsigma^{sys,t_{rnw}}_{CE,TD,IF} = \frac{\varsigma^{sys,t_{rnw}}_{TD,CE,O}}{\varsigma^{sys,t_{rnw}}_{SLSA,CE,O}} \quad (41)$$

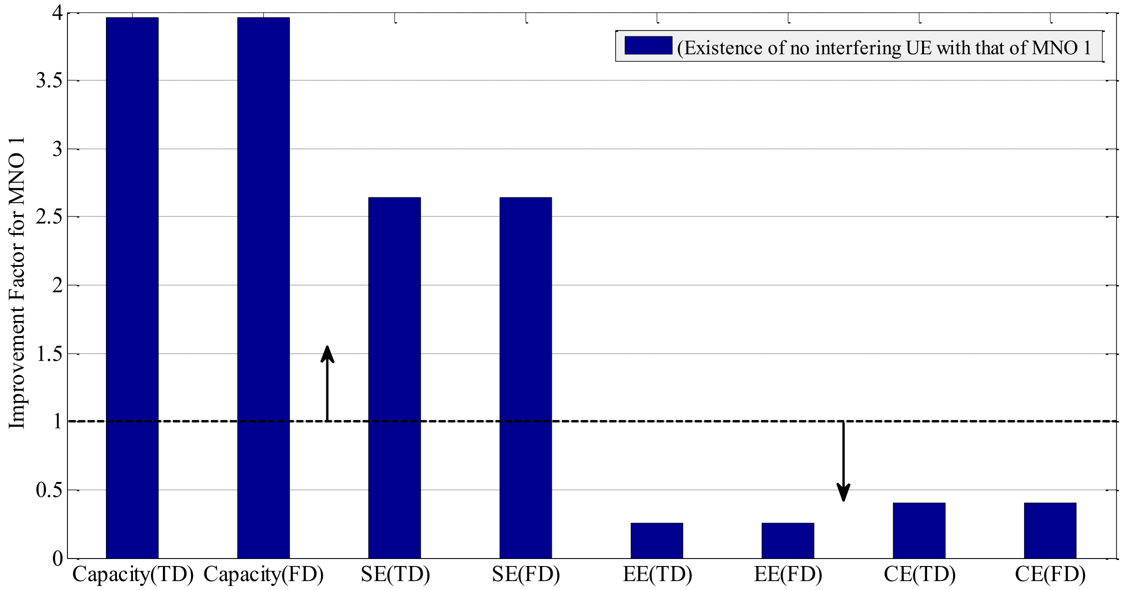

FIGURE 4. Improvement factors for MNO 1 in terms of average capacity, SE, EE, and CE when no interfering UE of other MNOs $\mathcal{O}\backslash o = 1$ exist with a small cell UE of MNO 1 in an apartment for $\varepsilon = 1$.

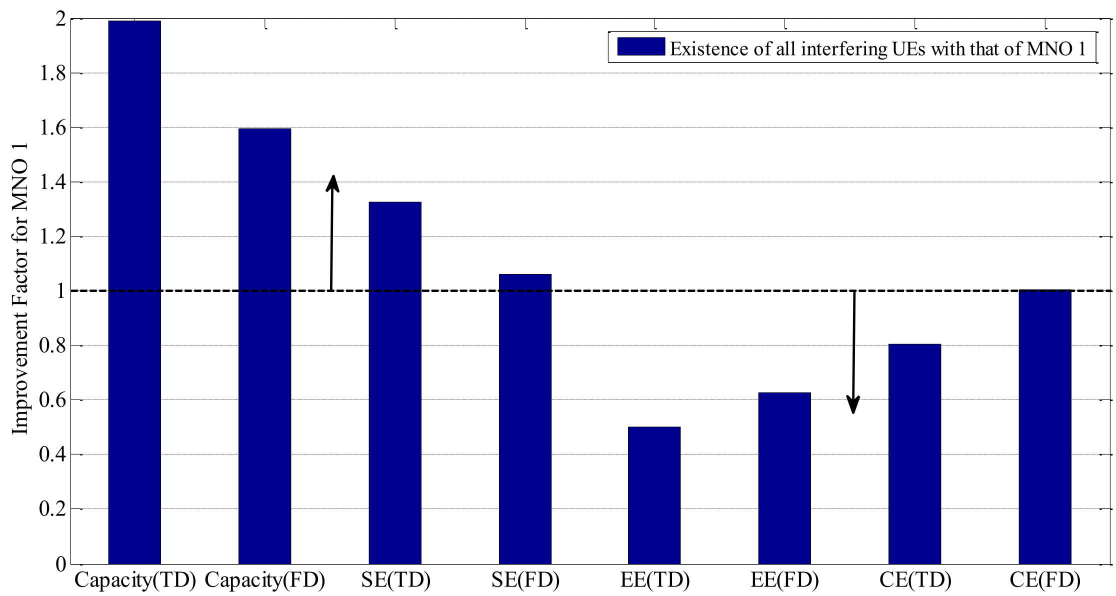

FIGURE 5. Improvement factors for MNO 1 in terms of average capacity, SE, EE, and CE when all interfering UE of other MNOs $\mathcal{O}\backslash o = 1$ exist with a small cell UE of MNO 1 in an apartment for $\varepsilon = 1$.

Similarly, when applying the proposed LCFSA technique with the frequency-domain CCI avoidance, the improvement factors for average capacity, SE, EE, and CE can be expressed respectively as follows.

$$\varsigma_{\text{cap,FD,IF}}^{\text{sys},t_{\text{rnw}}} = \frac{\sigma_{\text{FD,cap},\mathcal{O}}^{\text{sys},t_{\text{rnw}}}(L)}{\sigma_{\text{SLSA,cap},\mathcal{O}}^{\text{sys},t_{\text{rnw}}}(L)} \tag{42}$$

$$\varsigma_{\text{SE,FD,IF}}^{\text{sys},t_{\text{rnw}}} = \frac{\sigma_{\text{FD,SE},\mathcal{O}}^{\text{sys},t_{\text{rnw}}}(L)}{\sigma_{\text{SLSA,SE},\mathcal{O}}^{\text{sys},t_{\text{rnw}}}(L)} \tag{43}$$

$$\varsigma_{\text{EE,FD,IF}}^{\text{sys},t_{\text{rnw}}} = \frac{\sigma_{\text{FD,EE},\mathcal{O}}^{\text{sys},t_{\text{rnw}}}(L)}{\sigma_{\text{SLSA,EE},\mathcal{O}}^{\text{sys},t_{\text{rnw}}}(L)} \tag{44}$$

$$\varsigma_{\text{CE,FD,IF}}^{\text{sys},t_{\text{rnw}}} = \frac{\varsigma_{\text{FD,CE},\mathcal{O}}^{\text{sys},t_{\text{rnw}}}}{\varsigma_{\text{SLSA,CE},\mathcal{O}}^{\text{sys},t_{\text{rnw}}}} \tag{45}$$

IV. PERFORMANCE EVALUATION

A. DEFAULT PARAMETER, ASSUMPTION AND ESTIMATION

Table 1 shows the simulation parameters and assumptions used to evaluate the performance of the proposed LCFSA

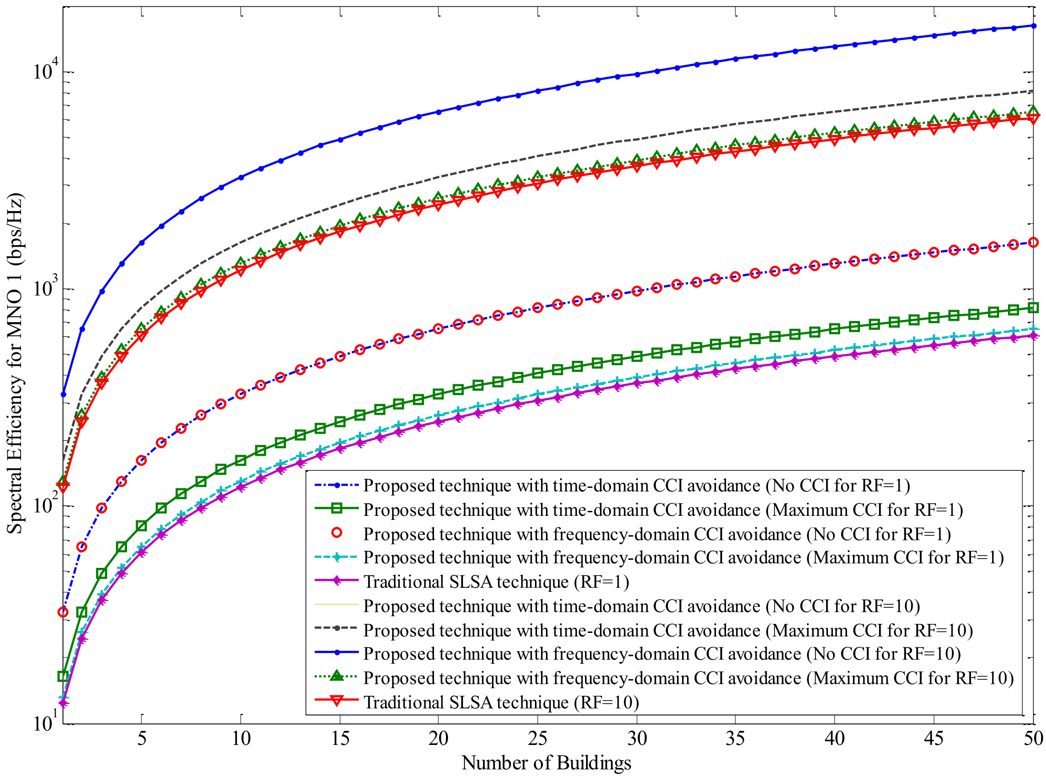

FIGURE 6. The impact of the variation in RF ε and L on the SE of MNO 1 when applying the proposed technique with the time-domain and frequency-domain CCI avoidance schemes.

technique both with the time-domain, as well as the frequency-domain, CCI avoidance schemes with respect to that of the traditional SLSA technique. MNOs 1, 2, 3, and 4 are assumed to have the number of subscribers of 40%, 30%, 20%, and 10% of $N_{C,\max,t_{rnw}}$ respectively at any term t_{rnw}.

If we consider only the first-tier of cSBSs in both the intra-floor and inter-floor levels and the double-sided cSBSs in the inter-floor level, we can then have $\lambda_{tra,1} = 8$ (Fig.1(c)) and $\lambda_{ter,1} = 2$ (Fig.1(b)). Following [33], $\alpha_f\left(d_{ter,1}\right) = 55$ dB. Now, using (8), $\left(2/I_{ter,1}\right) \ll \left(10^{5.5}\right)$ such that irrespective of the normalized value of $I_{ter,1} \leq 1$, $d_{ter,1}{}^* \geq d_0 = 1$ m is sufficient to reuse the same 28 GHz spectrum in the inter-floor level, where $d_0 = 1$ m is the minimum distance between an SBS and its serving UE. In other words, a minimum distance, which corresponds to $d_{ter,1}{}^* \geq d_0$, of 1 floor between cSBSs in the inter-floor level is sufficient to reuse the same mmWave spectrum. Note that the value of a floor height is considered as $d_f = 3$ m.

However, $d_{tra,1}{}^*$ decreases exponentially with an increase in the normalized value of $I_{tra,1} \leq 1$ [38]. Assume that $I_{tra,1} = 0.25$ such that using (7), we can find $d_{tra,1}{}^* = 34.4$ m, which corresponds to a minimum distance of at least 3 apartments between cSBSs in the intra-floor level. Note that the side length of a square apartment is considered as 10 m. Now, using (10)-(13), $\lambda_{cl,tra,1} = 9$ and $\lambda_{cl,ter,1} = 1$ such that the size of a 3D cluster of SBSs $\lambda_{cl,3D,1} = (9 \times 1) = 9$, which corresponds to a spectrum RF $\varepsilon_1 = \left(90/9\right) = 10$. Since we assume that each multistory building consists of 5 floors and there are 18 apartments per floor such that exactly one SBS per MNO is deployed within each apartment, the same countrywide full 28 GHz spectrum for MNO 1 can be reused to SBSs 2 times per floor and 10 times per building.

B. PERFORMANCE RESULT AND ANALYSIS

For the spectrum RF $\varepsilon = 1$ and a single building of SBSs (i.e., $l = 1$), the improvement factors for MNO 1 in terms of average capacity, SE, EE, and CE are shown in Fig.4 when no interfering UE, whereas in Fig.5 when all interfering UEs of other MNOs $\boldsymbol{O}\backslash o = 1$ exist with a small cell UE of MNO 1 in an apartment. It can be found from Fig.4 that the proposed LCFSA with both the time-domain and frequency-domain CCI avoidance schemes provide similar performance improvement in average capacity, SE, EE, and CE by about 296%, 164%, 75%, and 60% respectively over that of the traditional SLSA technique when no interfering UE exists (i.e., for no CCI) with a small cell UE of MNO 1. These improvements can be clarified by the fact that the traditional SLSA allocates an equal amount of 25% of the countrywide full 28 GHz spectrum to each of the four MNOs. This implies that MNO 1 can use a maximum of 25% of the countrywide full 28 GHz spectrum in each TTI of any $|\boldsymbol{T}| = Q = T_{APP}$ (i.e., 8 TTIs). In contrast, when no interfering UE exists with a small cell UE of MNO 1,

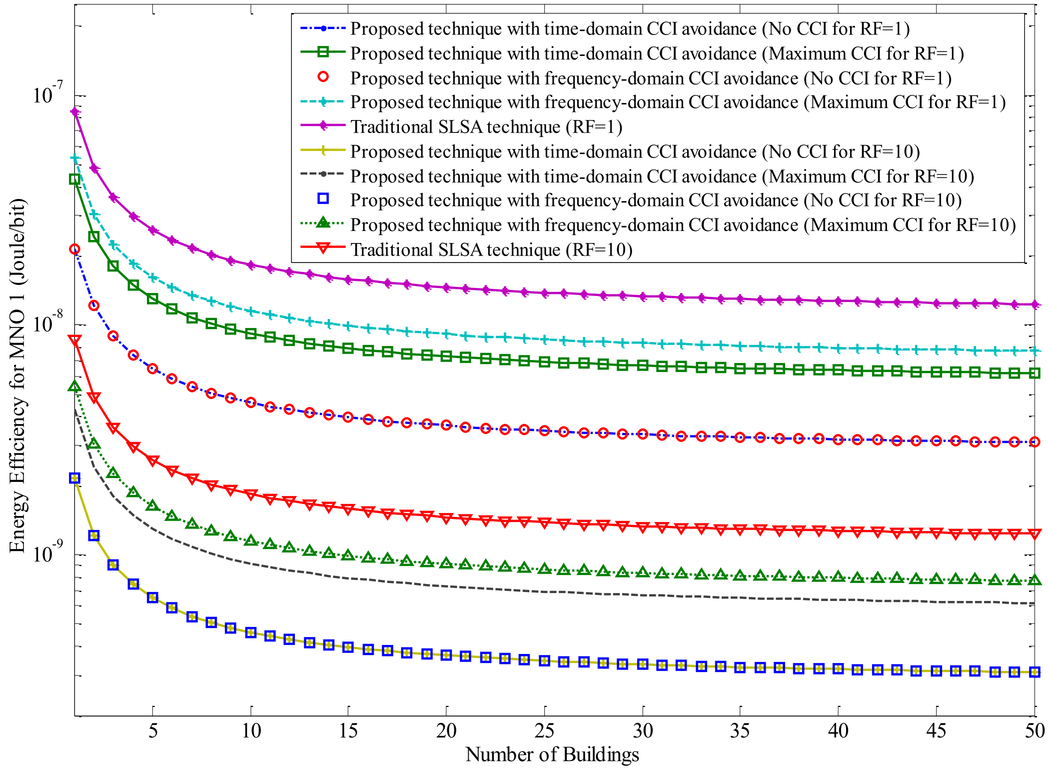

FIGURE 7. The impact of the variation in RF ε and L on the EE of MNO 1 when applying the proposed technique with the time-domain and frequency-domain CCI avoidance schemes.

the proposed LCFSA technique allows each MNO to access the countrywide full 28 GHz spectrum such that MNO 1 can now use the maximum of 100% of the countrywide full 28 GHz spectrum in each TTI of any $|\boldsymbol{T}| = Q = T_{\text{APP}}$ in both the time-domain and frequency-domain CCI avoidance schemes. Since the capacity and SE are directly proportional to the available spectrum of an MNO, the proposed technique improves both the capacity and SE performances. Likewise, EE and CE are inversely related to the achievable capacity such that an increase in capacity results in reducing the energy required per bit, as well as the cost of per bit/s.

However, when all interfering UEs of other MNOs $\boldsymbol{O}\backslash o = 1$ exist with a UE of MNO 1 in an apartment, MNO 1 can use the maximum of 100% of the countrywide full 28 GHz spectrum only in half of the total TTIs of any $|\boldsymbol{T}| = Q = T_{\text{APP}}$ (i.e., 4 TTIs) in the time-domain, and 40% of the countrywide full 28 GHz spectrum in each TTI of $|\boldsymbol{T}| = Q = T_{\text{APP}}$ (i.e., 8 TTIs) in the frequency-domain. Hence, from Fig.5, when all interfering UEs of other MNOs $\boldsymbol{O}\backslash o = 1$ exist with a UE of MNO 1 in an apartment, the proposed LCFSA with the time-domain improves average capacity, SE, EE, and CE by only about 99%, 32.5%, 50%, and 20% respectively, which also differ slightly from that with the frequency-domain (i.e., by about 59.2%, 6.1%, 37.2%, and 0.45% respectively). Note however that the reduction in improvement is due to the fact of the ceiling ${T^{\text{nABS}}_{1,t_{\text{rnw}},t_{\text{APP}}}}^*$ and ${M_{1,t_{\text{rnw},t}}}^*$ to their respective nearest integer values, and the impact of the ceiling error with ${T^{\text{nABS}}_{1,t_{\text{rnw}},t_{\text{APP}}}}^*$ is higher than that with ${M_{1,t_{\text{rnw},t}}}^*$. Since the proposed technique with the frequency-domain CCI avoidance scheme provides near actual values (i.e., fewer errors) in improvement factors for average capacity, SE, EE, and CE, the proposed LCFSA technique with the frequency-domain CCI avoidance scheme is preferable to the time-domain CCI avoidance scheme.

Figures 6 and 7 show the impact of the variation in RF and L on SE and EE performances respectively of the proposed technique. It can be found that both SE and EE improve with an increase in RF and L. Moreover, for any value of RF, SE increases linearly, whereas EE increases negatively exponentially with an increase in L. For any value of RF $\varepsilon > 1$ and $L > 1$, the SE and EE responses of the proposed LCFSA technique with the time-domain, as well as frequency-domain, CCI avoidance schemes vary similarly as in the case of RF $\varepsilon = 1$ and $L = 1$. For example, LCFSA with the time-domain CCI avoidance scheme for RF $\varepsilon = 10$ shows the best, whereas the traditional SLSA for RF $\varepsilon = 1$ shows the worst, SE and EE performances for any value of L. Note that due to the presence of RF and L both in the numerator (i.e., in LCFSA) and the denominator (i.e., in SLSA) in the expressions of average capacity, SE, EE, and CE performance improvement factors, the improvement factors of these metrics do not change with

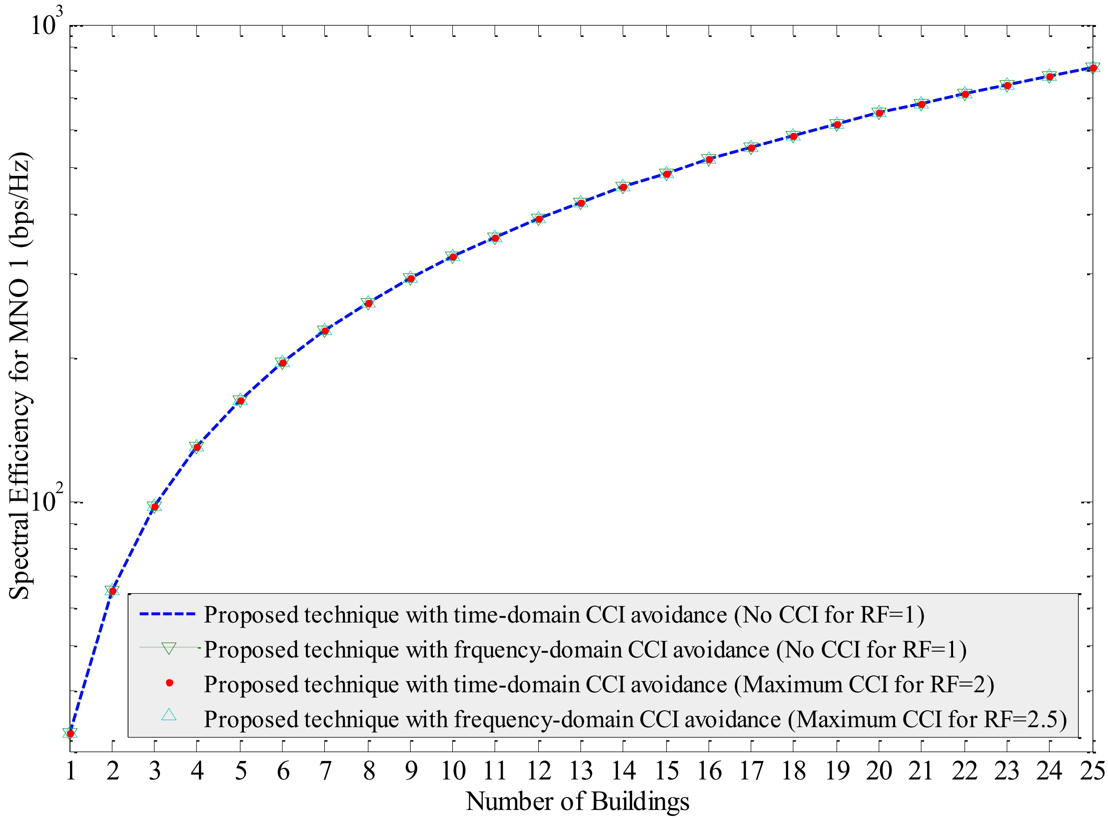

FIGURE 8. **Impact of varying RF ε on the improvement of the SE response of the proposed LCFSA technique with the time-domain, as well as the frequency-domain, CCI avoidance schemes in the worst-case CCI scenario.**

a change in RF and L, i.e. these metrics are independent of RF and L.

Since $(L \times \varepsilon \times \sigma^{t_{\text{rnw}}}_{\text{TD},o,l=1,\lambda_{\text{cl,3D}}}) \gg \sigma^{t_{\text{rnw}}}_{\text{MBS},o}$ and $(L \times \varepsilon \times \sigma^{t_{\text{rnw}}}_{\text{FD},o,l=1,\lambda_{\text{cl,3D}}}) \gg \sigma^{t_{\text{rnw}}}_{\text{MBS},o}$ (i.e., the aggregate capacity of macrocell UEs is very low as compared to that of small cell UEs in both the time-domain as well as the frequency domain, CCI avoidance schemes), the capacity can be expressed approximately as $\sigma^{\text{sys},t_{\text{rnw}}}_{\text{TD,cap},O}(L) \cong \sum_{o=1}^{O} (L \times \varepsilon \times \sigma^{t_{\text{rnw}}}_{\text{TD},o,l=1,\lambda_{\text{cl,3D}}})$ and $\sigma^{\text{sys},t_{\text{rnw}}}_{\text{FD,cap},O}(L) \cong \sum_{o=1}^{O} (L \times \varepsilon \times \sigma^{t_{\text{rnw}}}_{\text{FD},o,l=1,\lambda_{\text{cl,3D}}})$. Since $\sigma^{\text{sys},t_{\text{rnw}}}_{\text{TD,cap},O}(L)$ and $\sigma^{\text{sys},t_{\text{rnw}}}_{\text{FD,cap},O}(L)$ depend on $T^{\text{nABS}}_{1,t_{\text{rnw}},t_{\text{APP}}}{}^{*}$ and $M^{*}_{1,t_{\text{rnw},t}}$ respectively, each affected directly by the number of interfering UEs, by considering an appropriate value RF (i.e., ε) in a building, the CCI effect from interfering UEs of other MNOs $\boldsymbol{O}\backslash o = 1$ to an SBS of MNO 1 can be overcome. Hence, in the worst-case CCI, $T^{\text{nABS}}_{1,t_{\text{rnw}},t_{\text{APP}}}{}^{*} = 4$ TTIs and $M_{1,t_{\text{rnw},t}}{}^{*} = 80$ MHz for an observation time $Q = T_{\text{APP}} = 8$ TTIs and countrywide full 28 GHz mmWave spectrum $M_{\text{C,max}} = 200$ MHz. However, in the best case CCI (i.e., when no interfering UEs is present), MNO 1 can use $M_{\text{C,max}} = 200$ MHz for $Q = T_{\text{APP}} = 8$ TTIs. Hence, to overcome the CCI effect in the worst-case, the required value of RF in the time-domain is $\varepsilon = (8\,\text{TTIs}/4\,\text{TTIs}) = 2$, whereas in the frequency-domain is $\varepsilon = (200\text{ MHz}/80\text{ MHz}) = 2.5$. This can be found in Figs. 8 and 9, which show that the SE and EE responses of the proposed LCFSA technique with the time-domain CCI avoidance for the worst-case CCI for $\varepsilon = 2$, as well as with the frequency-domain CCI avoidance for the worst-case CCI for $\varepsilon = 2.5$ that coincide with their respective best-case CCI for $\varepsilon = 1$.

C. PERFORMANCE COMPARISON

According to [43], [44], it is expected that the future 6G mobile systems would require 10 times average SE (i.e., 270-370 bps/Hz) and 10 times average EE (i.e., 0.3×10^{-6} Joules/bit) of 5G [45], [46]. Considering 370 bps/Hz for the SE and 0.3 μJ/bit for the EE requirement for 6G, using Figs. 6 and 7, Table 2 shows that the proposed LCFSA technique can satisfy the SE and EE requirements for 6G with both the time-domain, as well as the frequency-domain, CCI avoidance schemes. Noticeably, satisfying both SE and EE requirements for 6G is dominated by the requirement of SE. Moreover, the worst-case CCI requires more reuse of the same countrywide full 28 GHz mmWave spectrum either intra-building level or inter-building level. In summary, depending on the deployment scenario of an operator's small cell networks indoors, the proposed LCFSA technique can satisfy the required SE and EE for 6G mobile systems by changing either RF ε or L, or both.

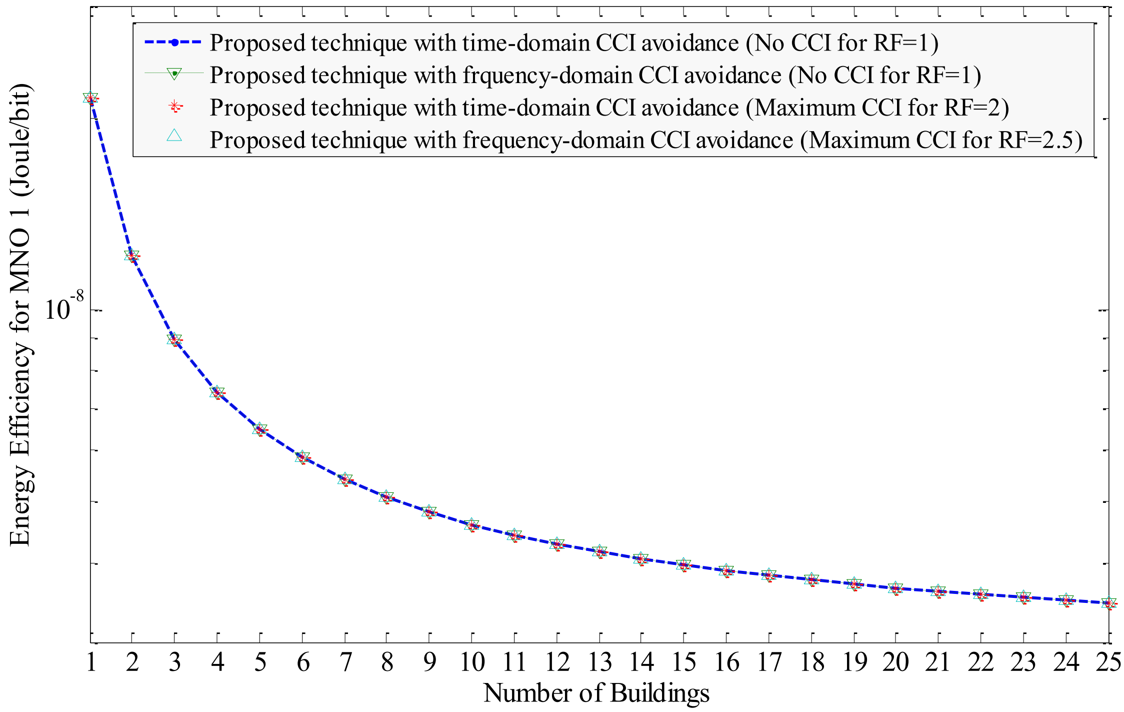

FIGURE 9. Impact of varying RF ε on the improvement of the SE response of the proposed LCFSA technique with the time-domain, as well as the frequency-domain, CCI avoidance schemes in the worst-case CCI scenario.

TABLE 2. L and RF ε requirements for the proposed LCFSA technique in both the time-domain and the frequency-domain for the best-case (B), as well as worst-case (W), CCI scenario for MNO 1 to fulfill average SE and EE requirements for 6G mobile systems.

ε	L											
	$SE \geq 270$ bps / Hz				$EE \leq 0.3$ μJ / bit				max(SE,EE)			
	TD		FD		TD		FD		TD		FD	
	B	W	B	W	B	W	B	W	B	W	B	W
1	12	24	12	29	1	1	1	1	12	24	12	29
10	2	3	2	3	1	1	1	1	2	3	2	3

V. CONCLUSION

In this paper, we have proposed a new technique for the spectrum allocation called licensed countrywide full-spectrum allocation (LCFSA) to allocate spectrum to mobile network operators (MNOs) in a country. Unlike the traditional static spectrum allocation technique that suffers from the insufficient spectrum availability and inefficient spectrum utilization due to allocating a portion of the licensed countrywide spectrum to each MNO in a country, the proposed LCFSA technique allocates the licensed countrywide full 28 GHz millimeter-wave (mmWave) spectrum to each MNO to operate its in-building small cells subject to avoiding CCI either in the time-domain or the frequency-domain such that both the spectrum availability and utilization can be increased. Because most mobile data are generated indoors, to address a large volume of data at high rates, the countrywide full mmWave spectrum allocated to an MNO is reused further to its in-building small cells.

Numerical analysis of CCI avoidance in both the time-domain and frequency-domain has been carried out to deduce the conditions for optimality in time and spectrum to serve user traffic demands of each MNO. We have derived average capacity, spectral efficiency (SE), energy efficiency (EE), and cost efficiency (CE) for the proposed LCFSA technique. We have then performed extensive numerical and simulation results and analyses for a country consisting of four MNOs for the existence of the maximum number of interfering UEs, as well as no interfering UE, with an SBS of an MNO in an apartment of a building.

It has been shown that the proposed LCFSA with both the time-domain and frequency-domain CCI avoidance schemes provide similar performance improvement in average capacity, SE, EE, and CE by about 296%, 164%, 75%, and 60% respectively over that of the traditional SLSA technique when no interfering UE exists (i.e., for no CCI) with a small cell UE of MNO 1. However, when all interfering UEs of other MNOs exist with a UE of MNO 1 in an apartment, the proposed LCFSA with the time-domain improves average capacity, SE, EE, and CE by only about 99%, 32.5%, 50%, and 20% respectively, whereas, with the frequency-domain, it improves by about 59.2%, 6.1%, 37.2%, and 0.45% respectively. These differences in responses with time-domain and frequency-domain have occurred due to the fact of the ceiling $T^{\mathrm{nABS}}_{1,t_{\mathrm{rnw}},t_{\mathrm{APP}}}{}^*$ and $M_{1,t_{\mathrm{rnw}},t}{}^*$ to their respective nearest integer values, and the impact of the ceiling error with $T^{\mathrm{nABS}}_{1,t_{\mathrm{rnw}},t_{\mathrm{APP}}}{}^*$ is higher than that with $M_{1,t_{\mathrm{rnw}},t}{}^*$ such that the proposed LCFSA technique with the frequency-domain CCI is preferable to the time-domain CCI avoidance scheme.

Moreover, due to the presence of RF and L both in the numerator and the denominator in the expressions of average capacity, SE, EE, and CE performance improvement factors, the improvement factors of these metrics do not change with a change in RF and L. Furthermore, by adjusting RF, the impact of interfering UEs, particularly in the worst-case CCI scenario can be compensated. Finally, we have shown that the proposed LCFSA technique can satisfy SE and EE requirements for 6G systems by adjusting either RF ε or L, or both. Hence, depending on the deployment scenario of an operator's small cell networks indoors, the proposed LCFSA technique can satisfy the required SE and EE for 6G mobile systems by changing either RF ε or L or both.

ACKNOWLEDGMENT

This article has been presented in part at the 2020 IEEE 92nd Vehicular Technology Conference (VTC2020-Fall), Victoria, BC, Canada, October 4–7, 2020.

REFERENCES

[1] S. Rangan, T. S. Rappaport, and E. Erkip, "Millimeter-wave cellular wireless networks: Potentials and challenges," *Proc. IEEE*, vol. 102, no. 3, pp. 366–385, Mar. 2014, doi: 10.1109/JPROC.2014.2299397.

[2] S. Jin, W. Tan, M. Matthaiou, J. Wang, and K.-K. Wong, "Statistical eigenmode transmission for the MU-MIMO downlink in rician fading," *IEEE Trans. Wireless Commun.*, vol. 14, no. 12, pp. 6650–6663, Dec. 2015, doi: 10.1109/TWC.2015.2457900.

[3] A. Sayeed and J. Brady, "Beamspace MIMO for high-dimensional multiuser communication at millimeter-wave frequencies," in *Proc. IEEE Global Commun. Conf. (GLOBECOM)*, Atlanta, GA, USA, Dec. 2013, pp. 3679–3684.

[4] T. S. Rappaport, S. Sun, R. Mayzus, H. Zhao, Y. Azar, K. Wang, G. N. Wong, J. K. Schulz, M. Samimi, and F. Gutierrez, "Millimeter wave mobile communications for 5G cellular: It will work!," *IEEE Access*, vol. 1, pp. 335–349, 2013, doi: 10.1109/ACCESS.2013.2260813.

[5] T. E. Bogale and L. B. Le, "Massive MIMO and mmWave for 5G wireless HetNet: Potential benefits and challenges," *IEEE Veh. Technol. Mag.*, vol. 11, no. 1, pp. 64–75, Mar. 2016, doi: 10.1109/MVT.2015.2496240.

[6] C. Tsinos, A. Galanopoulos, and F. Foukalas, "Low-complexity and low-feedback-rate channel allocation in CA MIMO systems with heterogeneous channel feedback," *IEEE Trans. Veh. Technol.*, vol. 66, no. 5, pp. 4396–4409, May 2017, doi: 10.1109/TVT.2016.2609539.

[7] M. Neri, M.-G. Di Benedetto, T. Pecorella, C. Carlini, A. Castellani, P. Obino, and P. Sciarratta, "Ultra-broadband mobile networks from LTE-advanced to 5G: Evaluation of massive MIMO and multi-carrier aggregation effectiveness," in *Proc. AEIT Int. Annu. Conf.*, Cagliari, Italy, Sep. 2017, pp. 1–6.

[8] M. S. Ayub, L. Wuttisittikulkij, P. Adasme, and I. Soto, "Hybrid precoding design for two carriers aggregated in 5G massive MIMO system," in *Proc. South Amer. Colloq. Visible Light Commun. (SACVC)*, Santiago, Chile, Jun. 2020, pp. 1–5.

[9] G. Yuan, X. Zhang, W. Wang, and Y. Yang, "Carrier aggregation for LTE-advanced mobile communication systems," *IEEE Commun. Mag.*, vol. 48, no. 2, pp. 88–93, Feb. 2010, doi: 10.1109/MCOM.2010.5402669.

[10] C. M. Park, H. B. Jung, S. H. Kim, and D. K. Kim, "System level performance evaluation of various carrier aggregation scenarios in LTE-advanced," in *Proc. ICACT*, Pyeong Chang, 2013, pp. 814–817.

[11] D. P. Sharma and S. K. Gautam, "Distributed and prioritised scheduling to implement carrier aggregation in LTE advanced systems," in *Proc. 4th Int. Conf. Adv. Comput. Commun. Technol.*, Rohtak, India, Feb. 2014, pp. 390–393.

[12] N. Lei, C. Guo, C. Feng, and Y. Chen, "A multi-user MIMO resource scheduling scheme for carrier aggregation scenario," in *Proc. Int. Conf. Wireless Commun. Signal Process. (WCSP)*, Nanjing, China, Nov. 2011, pp. 1–5.

[13] M. Wang, F. Gao, S. Jin, and H. Lin, "An overview of enhanced massive MIMO with array signal processing techniques," *IEEE J. Sel. Topics Signal Process.*, vol. 13, no. 5, pp. 886–901, Sep. 2019, doi: 10.1109/JSTSP.2019.2934931.

[14] P. Liu, S. Jin, T. Jiang, Q. Zhang, and M. Matthaiou, "Pilot power allocation through user grouping in multi-cell massive MIMO systems," *IEEE Trans. Commun.*, vol. 65, no. 4, pp. 1561–1574, Apr. 2017, doi: 10.1109/TCOMM.2016.2645767.

[15] R. K. Saha, P. Saengudomlert, and C. Aswakul, "Evolution toward 5G mobile networks – a survey on enabling technologies," *Eng. J.*, vol. 20, no. 1, pp. 87–119, Jan. 2016, doi: 10.4186/ej.2016.20.1.87.

[16] T. L. Marzetta, "Noncooperative cellular wireless with unlimited numbers of base station antennas," *IEEE Trans. Wireless Commun.*, vol. 9, no. 11, pp. 3590–3600, Nov. 2010, doi: 10.1109/TWC.2010.092810.091092.

[17] D. Qiao, Y. Wu, and Y. Chen, "Massive MIMO architecture for 5G networks: Co-located, or distributed?" in *Proc. 11th Int. Symp. Wireless Commun. Syst. (ISWCS)*, Barcelona, Spain, Aug. 2014, pp. 192–197.

[18] W. Roh, J.-Y. Seol, J. Park, B. Lee, J. Lee, Y. Kim, J. Cho, K. Cheun, and F. Aryanfar, "Millimeter-wave beamforming as an enabling technology for 5G cellular communications: Theoretical feasibility and prototype results," *IEEE Commun. Mag.*, vol. 52, no. 2, pp. 106–113, Feb. 2014, doi: 10.1109/MCOM.2014.6736750.

[19] J. G. Andrews, S. Buzzi, W. Choi, S. V. Hanly, A. Lozano, A. C. K. Soong, and J. C. Zhang, "What will 5G be?" *IEEE J. Sel. Areas Commun.*, vol. 32, no. 6, pp. 1065–1082, Jun. 2014, doi: 10.1109/JSAC.2014.2328098.

[20] R. C. Daniels and R. W. Heath, "60 GHz wireless communications: Emerging requirements and design recommendations," *IEEE Veh. Technol. Mag.*, vol. 2, no. 3, pp. 41–50, Sep. 2007, doi: 10.1109/MVT.2008.915320.

[21] A. F. Cattoni, H. T. Nguyen, J. Duplicy, D. Tandur, B. Badic, R. Balraj, F. Kaltenberger, I. Latif, A. Bhamri, G. Vivier, I. Z. Kovacsk, and P. Horvath, "Multi-user MIMO and carrier aggregation in 4G systems: The SAMURAI approach," in *Proc. IEEE Wireless Commun. Netw. Conf. Workshops (WCNCW)*, Paris, France, Apr. 2012, pp. 288–293.

[22] H. Mizutani, R. Ishikawa, and K. Honjo, "A novel Sub-6-GHz and 28-GHz GaN switchable diplexer MMIC for carrier aggregation with massive MIMO full duplex link," in *Proc. IEEE Asia–Pacific Microw. Conf. (APMC)*, Singapore, Dec. 2019, pp. 1429–1431.

[23] A. Farhang, N. Marchetti, L. E. Doyle, and B. Farhang-Boroujeny, "Filter bank multicarrier for massive MIMO," in *Proc. IEEE 80th Veh. Technol. Conf. (VTC-Fall)*, Vancouver, BC, Canada, Sep. 2014, pp. 1–7.

[24] Y. Xing, R. Chandramouli, and C. Cordeiro, "Price dynamics in competitive agile spectrum access markets," *IEEE J. Sel. Areas Commun.*, vol. 25, no. 3, pp. 613–621, Apr. 2007, doi: 10.1109/JSAC.2007.070411.

[25] D. Niyato, E. Hossain, and Z. Han, "Dynamics of multiple-seller and multiple-buyer spectrum trading in cognitive radio networks: A game-theoretic modeling approach," *IEEE Trans. Mobile Comput.*, vol. 8, no. 8, pp. 1009–1022, Aug. 2009, doi: 10.1109/TMC.2008.157.

[26] F. Hu, B. Chen, J. Wang, M. Li, P. Li, and M. Pan, "MastDP: Matching based double auction mechanism for spectrum trading with differential privacy," in *Proc. IEEE Global Commun. Conf. (GLOBECOM)*, Waikoloa Village, HI, USA, Dec. 2019, pp. 1–6.

[27] M. K. Farshbafan, M. H. Bahonar, and F. Khaiehraveni, "Spectrum trading for Device-to-Device communication in cellular networks using incomplete information bandwidth-auction game," in *Proc. 27th Iranian Conf. Electr. Eng. (ICEE)*, Yazd, Iran, Apr. 2019, pp. 1441–1447.

[28] R. K. Saha, "A technique for massive spectrum sharing with ultra-dense in-building small cells in 5G era," in *Proc. IEEE VTC-Fall*, Honolulu, HI, USA, 2019, pp. 1–7.

[29] R. K. Saha, "Countrywide mobile spectrum sharing with small indoor cells for massive spectral and energy efficiencies in 5G and beyond mobile networks," *Energies*, vol. 12, no. 20, p. 3825, Oct. 2019, doi: 10.3390/en12203825.

[30] R. H. Tehrani, S. Vahid, D. Triantafyllopoulou, H. Lee, and K. Moessner, "Licensed spectrum sharing schemes for mobile operators: A survey and outlook," *IEEE Commun. Surveys Tuts.*, vol. 18, no. 4, pp. 2591–2623, 4th Quart., 2016, doi: 10.1109/COMST.2016.2583499.

[31] M. L. Attiah, A. A. M. Isa, Z. Zakaria, M. K. Abdulhameed, M. K. Mohsen, and I. Ali, "A survey of mmWave user association mechanisms and spectrum sharing approaches: An overview, open issues and challenges, future research trends," *Wireless Netw.*, vol. 26, no. 4, pp. 2487–2514, May 2020, doi: 10.1007/s11276-019-01976-x.

[32] S. K. Joshi, K. B. S. Manosha, M. Codreanu, and M. Latva-aho, "Dynamic inter-operator spectrum sharing via Lyapunov optimization," *IEEE Trans. Wireless Commun.*, vol. 16, no. 10, pp. 6365–6381, Oct. 2017, doi: 10.1109/TWC.2017.2722999.

[33] R. K. Saha, "Modeling interference to reuse millimeter-wave spectrum to in-building small cells toward 6G," in *Proc. IEEE VTC-Fall*, Victoria, BC, Canada, 2020, pp. 1–6.

[34] N. Saquib, E. Hossain, and D. Kim, "Fractional frequency reuse for interference management in LTE-advanced hetnets," *IEEE Wireless Commun.*, vol. 20, no. 2, pp. 113–122, Apr. 2013, doi: 10.1109/MWC.2013.6507402.

[35] R. A. Hassan, A. Idris, H. Adto, M. Ramadhan, and M. Kassim, "Reduction of inter-cell interference in close proximity cell using dynamic fractional frequency reuse method," in *Proc. IEEE Conf. Syst., Process Control (ICSPC)*, Malacca, Malaysia, Dec. 2017, pp. 157–161.

[36] R. K. Saha, "A hybrid system and technique for sharing multiple spectrums of satellite plus mobile systems with indoor small cells in 5G and beyond era," *IEEE Access*, vol. 7, pp. 77569–77596, 2019, doi: 10.1109/ACCESS.2019.2921723.

[37] R. K. Saha and C. Aswakul, "A novel frequency reuse technique for in-building small cells in dense heterogeneous networks," *IEEJ Trans. Electr. Electron. Eng.*, vol. 13, no. 1, pp. 98–111, Jan. 2018, doi: 10.1002/tee.22503.

[38] R. K. Saha, "3D spatial reuse of Multi-Millimeter-Wave spectra by ultra-dense in-building small cells for spectral and energy efficiencies of future 6G mobile networks," *Energies*, vol. 13, no. 7, p. 1748, Apr. 2020, doi: 10.3390/en13071748.

[39] *Evolved Universal Terrestrial Radio Access (E-UTRA); Radio Frequency (RF) System Scenarios*, document 3GPP TR 36.942, V.1.2.0, 3rd Generation Partnership Project, Jul. 2007. Accessed: Feb. 15, 2020. [Online]. Available: https://portal.3gpp.org/ desktopmodules /Specifications/Specification Details.aspx?specificationId=2592

[40] *Simulation Assumptions and Parameters for FDD HeNB RF Requirements*, document TSG RAN WG4 (Radio) Meeting #51, R4-092042, 3GPP, May 2009. Accessed: Feb. 13, 2020. [Online]. Available: https://www.3gpp.org/ftp/tsg_ran /WG4_Radio/TSGR4_51/Documents/

[41] *Guidelines for Evaluation of Radio Interface Technologies for IMT-2020*, document ITU-R M.2412-0, Geneva, Switzerland, Oct. 2017. Accessed: Feb. 13, 2020. [Online]. Available: https://www.itu.int/dms_pub/itu-r/opb/rep/R-REP-M.2412-2017-PDF-E.pdf

[42] G. R. Maccartney, T. S. Rappaport, S. Sun, and S. Deng, "Indoor office wideband millimeter-wave propagation measurements and channel models at 28 and 73 GHz for ultra-dense 5G wireless networks," *IEEE Access*, vol. 3, pp. 2388–2424, 2015, doi: 10.1109/ACCESS.2015.2486778.

[43] Z. Zhang, Y. Xiao, Z. Ma, M. Xiao, Z. Ding, X. Lei, G. K. Karagiannidis, and P. Fan, "6G wireless networks: Vision, requirements, architecture, and key technologies," *IEEE Veh. Technol. Mag.*, vol. 14, no. 3, pp. 28–41, Sep. 2019, doi: 10.1109/MVT.2019.2921208.

[44] S. Chen, Y.-C. Liang, S. Sun, S. Kang, W. Cheng, and M. Peng, "Vision, requirements, and technology trend of 6G: How to tackle the challenges of system coverage, capacity, user data-rate and movement speed," *IEEE Wireless Commun.*, vol. 27, no. 2, pp. 218–228, Apr. 2020, doi: 10.1109/MWC.001.1900333.

[45] C.-X. Wang, F. Haider, X. Gao, X.-H. You, Y. Yang, D. Yuan, H. Aggoune, H. Haas, S. Fletcher, and E. Hepsaydir, "Cellular architecture and key technologies for 5G wireless communication networks," *IEEE Commun. Mag.*, vol. 52, no. 2, pp. 122–130, Feb. 2014, doi: 10.1109/MCOM.2014.6736752.

[46] G. Auer, V. Giannini, C. Desset, I. Godor, P. Skillermark, M. Olsson, M. Imran, D. Sabella, M. Gonzalez, O. Blume, and A. Fehske, "How much energy is needed to run a wireless network?" *IEEE Wireless Commun.*, vol. 18, no. 5, pp. 40–49, Oct. 2011, doi: 10.1109/MWC.2011.6056691.

[47] R. K. Saha, "A countrywide licensed full spectrum allocation method for millimeter-wave mobile systems for 6G," in *Proc. IEEE VTC-Fall Workshops*, Victoria, BC, Canada, 2020, pp. 1–7.

RONY KUMER SAHA received the B.Sc. degree in electrical and electronic engineering from the Khulna University of Engineering and Technology, KUET, in 2004, the M.Eng. degree in information and communications technologies from the Asian Institute of Technology (AIT), Thailand, in 2011, and the Ph.D. degree in electrical engineering from Chulalongkorn University, Thailand, in 2017.

He worked as a Lecturer and later promoted to an Assistant Professor with American International University-Bangladesh (AIUB), Bangladesh, from January 2005 to August 2013. From September 2013 to July 2014, he was with East West University, Bangladesh. Since 2017, he has been working as a Research Engineer with the Radio and Spectrum Laboratory, KDDI Research, Inc., Japan. His current research interests include 5G and beyond ultra-dense HetNets, spectrum sharing, policy, and management in multiple communication systems, and millimeter-wave communications. He has research experiences on mobile wireless communications in universities and industries for more than ten years. He has authored about 50 peer-reviewed, reputed, and highly recognized international journals [e.g., IEEE Access, *IJCS* (Wiley), *Sensors* (MDPI), *Energies* (MDPI), and *IEEJ* (Wiley)] and conferences (the IEEE ICC, the IEEE GLOBECOM, the IEEE PIMRC, the IEEE VTC, the IEEE DySPAN, WPMC, ICSNC, and ECTI-CON) papers. He also filed an international patent.

Dr. Saha has served as a member for the Fronthaul Working Group, xRAN Forum, USA. He has also served as a TPC Member for the 2018 IEEE Global Communications Conference Workshops and The Fifteenth International Conference on Systems and Networks Communications (ICSNC), Porto, Portugal, October 2020. Furthermore, he has also served as the Session Chair for two sessions, namely Radio Resource Management and Aerial Networks at 2019 IEEE VTC-Fall, Hawaii, USA, as well as the 2019 IEEE International Symposium on Dynamic Spectrum Access Networks Newark, NJ, USA, for the session Spectrum Sharing in 5G. Since early 2019, he has been serving as an Associate Editor for the *Engineering Journal*, Thailand. He has served as a Reviewer for a number of recognized journals, including the IEEE Transactions on Vehicular Technology, IEEE Access, *Physical Communication* (Elsevier), the *International Journal of Communication Systems* (Wiley), *Sensors Journal* (MDPI), *Symmetry Journal* (MDPI), *Mobile Information Systems* (Hindawi), and *Sustainability Journal* (MDPI).